Earth and Planetary Science Letters 409 (2015) 133–146

Contents lists available at ScienceDirect

Earth and Planetary Science Letters

www.elsevier.com/locate/epsl

Frontiers paper

The surge of great earthquakes from 2004 to 2014

Thorne Lay *

Department of Earth and Planetary Sciences, University of California Santa Cruz, Santa Cruz, CA 95064, USA

ARTICLE INFO

Article history:
Received 22 August 2014
Received in revised form 25 October 2014
Accepted 28 October 2014
Available online xxxx
Editor: M.M. Hirschmann

Keywords:
great earthquakes
rupture processes
earthquake triggering

ABSTRACT

During the decade from mid-2004 to mid-2014 18 great ($M_w \geq 8.0$) earthquakes occurred globally (~1.8 per year), compared to 71 from 1900 to mid-2004 (~0.68 per year), yielding a short-term rate increase of 265%. Six events had $M_w \geq 8.5$, larger than any prior event since the 1965 Rat Islands earthquake. The December 26, 2004 M_w 9.2 Sumatra earthquake had the longest recorded rupture length of 1300+ km and a rupture duration exceeding 450 s. The largest recorded strike-slip earthquake (M_w 8.7) occurred in the Indo–Australian plate on April 11, 2012. The largest recorded deep focus earthquake (M_w 8.3) occurred under the Sea of Okhotsk on May 24, 2013. While this overall surge of activity has not been demonstrated to be causally linked, regional spatio-temporal clustering is clearly evident for great events along the Sumatra, Kuril and Tonga subduction zones, and longer-range interactions have been established for global seismicity and seismic tremor at lower magnitudes following some of the events. This recent decade of intense great earthquake activity coincided with vastly expanded global networks of seismometers, GPS stations, tsunami gauges, and new satellite imaging capabilities such as InSAR and LandSAT interferometry and gravity measurements by GRACE and GOCE, enabling unprecedented analyses of precursory, co-seismic and post-seismic processes around the subduction zone environments where most of the events occurred. Individual events such as the March 11, 2011, Tohoku, Japan M_w 9.0 earthquake produced more ground motion and tsunami recordings than available for all great earthquakes of the last century collectively. Joint inversion and modeling of the diverse data sets exploit complementary sensitivity of the signals to different aspects of the earthquake processes. Major advances have been achieved in quantifying frictional locking and strain accumulation prior to some great events and in relating it to co-seismic slip heterogeneity. Many surprising aspects of these well-quantified great earthquakes have been manifested, associated with their rupture dimensions, tectonic location, compound faulting, triggering interactions, slow slip and foreshock migration precursors, aftershock complexity, and depth-varying seismic radiation characteristics. Regions with potential for near-future great ruptures include mature seismic gaps along the Mentawai Islands and northern Chile, as well as western North America and the Himalayan front, so more great earthquake activity can certainly be anticipated.

1. Introduction

Plate tectonics causes earthquakes of all sizes, but usually the most significant events in terms of both hazards and tectonic motions are "great" earthquakes, classically defined as those with seismic magnitudes ≥8.0. For the seismic energy-based moment magnitude M_w (Kanamori, 1977) this corresponds to events with seismic moments $M_0 \geq 1.26 \times 10^{21}$ Nm. There is nothing particularly significant about this value in the continuum of earthquake size, but for this study the focus will primarily be on great earthquakes as a convenient threshold for discussion.

Over the time interval of seismological recording and reliable measurement of earthquake size from seismic waves dating from about 1900 to present, there have been about 89 great earthquakes around the world. This number is taken from the U.S. Geological Survey National Earthquake Information Center bulletin (USGS-NEIC: http://earthquake.usgs.gov/earthquakes/map/), which draws upon the PAGER-CAT compilation for events prior to 1973 (Allen et al., 2009). Magnitudes of events early in the 20th century are uncertain due to sparseness of observations, uncertain instrument responses, and variable measurement procedures, whereas the modern events that are discussed here have relatively robustly determined seismic moments and M_w.

Fig. 1 shows locations of great earthquakes around the Pacific and Indian Ocean subduction zones from 1900 to present,

* Tel.: +1 831 459 3164.
E-mail address: tlay@ucsc.edu.

http://dx.doi.org/10.1016/j.epsl.2014.10.047
0012-821X/

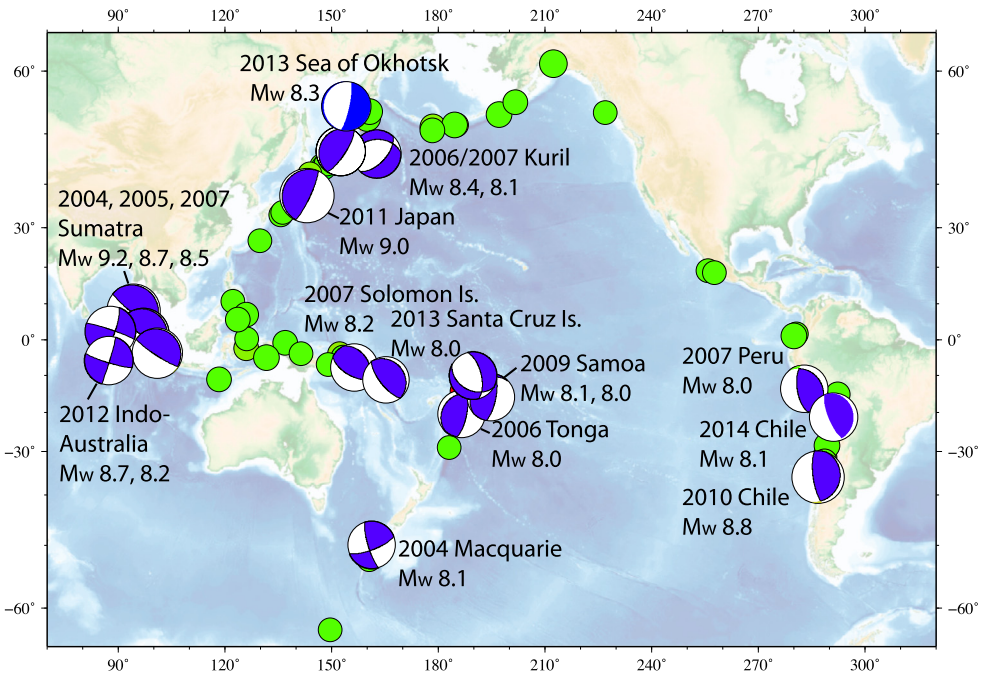

Fig. 1. Locations of 89 great ($M_w \geq 8.0$) earthquakes from 1900–2014 (green circles), with the 18 labeled events from 2004 to 2014 being depicted with lower hemisphere focal mechanisms for the best double-couple geometry of the corresponding global centroid-moment tensor (GCMT) solutions for all except the triggered M_w 8.0 thrust event of the 2009 Samoa Islands doublet (Lay et al., 2010c).

with focal mechanisms included for all recent events from December 2004 to April 2014. The latter are the best-double couple solutions for the corresponding global centroid-moment tensor (GCMT) inversions (http://www.globalcmt.org/CMTsearch.html) for these events with one exception being for a triggered thrust event in Tonga that overlapped the 2009 Samoa normal-faulting earthquake (Lay et al., 2010c). The recent great events have been widespread, occurring in close proximity to subduction zones that have hosted the majority of earlier great events (Fig. 1). 11 of the 18 recent events have been located on interplate megathrust faults, two are normal-faulting events that ruptured near the outer rise in subducting Pacific plate, three are strike-slip events located seaward of a plate boundary, one (May 3, 2006, Tonga) is a 65 km deep intraslab event, and one (May 24, 2013, Sea of Okhotsk) is 610 km deep in the subducted Pacific slab. The megathrust faulting events along Chile, Peru, Kuril Islands, Japan, Sumatra, Solomon Islands and Santa Cruz Islands all struck regions that were recognized as seismic gaps or zones of uncertain earthquake potential to varying degree (e.g., Nishenko, 1991); the other events have far less clear tectonic frameworks for having anticipated the size and style of faulting involved.

The time sequence for global earthquakes with magnitudes greater than 7.5 from 1900 to 2014 is shown in Fig. 2a. The magnitude used here is the PAGER-CAT preferred magnitude (M) for events prior to 1976 and GCMT M_w for subsequent events other than for several preferred results from finite-fault modeling solutions. Ammon et al. (2010) show that the running decadal average of events with magnitudes $\geq$7.5 (or 8.0, but not for 7.0) is greater for the most recent decade than for any prior decade in the seismological interval from 1900 to present. The interval from 1950 to 1965 experienced 13 great earthquakes, including the 1960 Chile ($M_w \sim 9.5$) and 1964 Alaska ($M_w \sim 9.2$) events, which are the two largest seismologically-recorded events.

This short seismological record appears inadequate for reliably evaluating statistical significance of clustering or interaction of great events, although efforts to do so generally indicate that the data cannot rule out a random Poissonian distribution

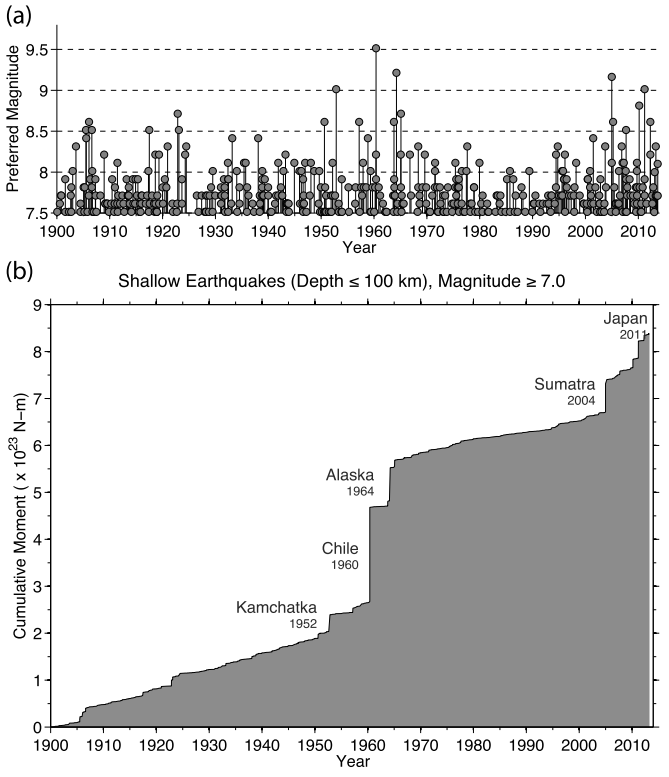

Fig. 2. (a) Time sequence of global large earthquakes with preferred magnitudes, $M \geq 7.5$ from the NEIC-PAGER catalog, for the seismological record from 1900 to 2014. (b) Cumulative seismic moment for earthquakes with hypocentral depths less than 100 km with $M \geq 7.0$ from 1900 to 2014 using moment estimates listed in the USGS NEIC-PAGER catalog. Large increases due to events with $M_w \geq 9.0$ are labeled. Modified from Ammon et al. (2010), courtesy of Charles J. Ammon.

of events, after conventionally defined aftershocks are removed (e.g., Michael, 2011; Daub et al., 2012; Parsons and Geist, 2012; Shearer and Stark, 2012; Ben-Naim et al., 2013), although there

are differing interpretations (e.g., Bufe and Perkins, 2011; Thenhaus et al., 2011). At the same time, there is quite compelling evidence for recent great earthquakes producing dynamic triggering of small events on a global scale during passage of surface waves (e.g., West et al., 2005; Velasco et al., 2008; Parsons and Velasco, 2011; Gonzalez-Huizar et al., 2012), as well as somewhat more ambiguous delayed intervals of rate increases (Pollitz et al., 2012; Gonzalez-Huizar et al., 2012). Attempts to detect physical connections between delayed remote events in the form of dynamically-triggered seismicity rate increases at sites of future great events coincident with passage of seismic waves from earlier great events have not established statistically robust interactions (e.g., van der Elst et al., 2013).

Cumulative seismic moment for large earthquakes around the world is still dominated by the great events of the 1960s (Fig. 2b), but the high rate of great earthquakes in the recent decade has resulted in the steepest sustained slope of cumulative seismic moment otherwise. Scientifically, the clearest importance of this recent high rate of activity is that it has overlapped an interval of greatly expanded global deployment of geophysical instrumentation (Ammon et al., 2010) that has captured seismic, geodetic, and tsunami signals generated by the numerous large events, allowing unprecedented investigation of their rupture processes and associated precursory and post-seismic deformation.

2. Great earthquake surprises

The recent spate of great earthquakes has provided sobering demonstrations of our limited understanding of large earthquake ruptures. This is not particularly unexpected given the short observation period for which we have acquired quantitative recordings of earthquakes, but it cautions us against placing high confidence in conceptual models that have been developed based on that limited information base. A brief consideration of the great events in several regions highlights some of the surprises.

Sumatra region

The December 26, 2004 Sumatra M_w 9.2 earthquake (Fig. 3) ruptured for more than 450 s along an unprecedented fault length totaling 1300+ km along the Sumatra–Andaman subduction zone (e.g., Lay et al., 2005; Ammon et al., 2005; Vigny et al., 2005; Banerjee et al., 2007; Chlieh et al., 2007; Rhie et al., 2007; Shearer and Bürgmann, 2010). The duration of faulting caused most finite-fault modeling procedures in use at the time to fail, prompting extensive upgrades of modeling capabilities to account for overlapping body wave arrivals within such a long rupture duration (Ammon et al., 2005). Underthrusting-motion extended along the curved, oblique-convergence plate boundary into a region ~1000 km long where relative plate motion is predominantly trench-parallel. The rupture traversed much smaller historical rupture zones of events in 1847, 1881 and 1941 in the Nicobar and Andaman Islands regions (Fig. 3), negating any strong segmentation of that part of the plate boundary. Tsunami observations were very limited for the 2004 event, but available data, including sea level altimetry data helped to constrain the rupture length and along-dip slip distribution (e.g., Lay et al., 2005; Fujii and Satake, 2007; Poisson et al., 2011)

Less surprising was the regional activation of adjacent great underthrusting ruptures along Sumatra on March 28, 2005 (M_w 8.6) (Briggs et al., 2006; Banerjee et al., 2007; Konca et al., 2007) and September 12, 2007 (M_w 8.5) (Konca et al., 2008), given the long intervals of strain accumulation since prior failures of the plate boundary in those regions in 1861 and 1833, respectively (Fig. 3). This spatio-temporal clustering of great events is similar to that observed along the Alaska–Aleutians arc from 1957–1965. While

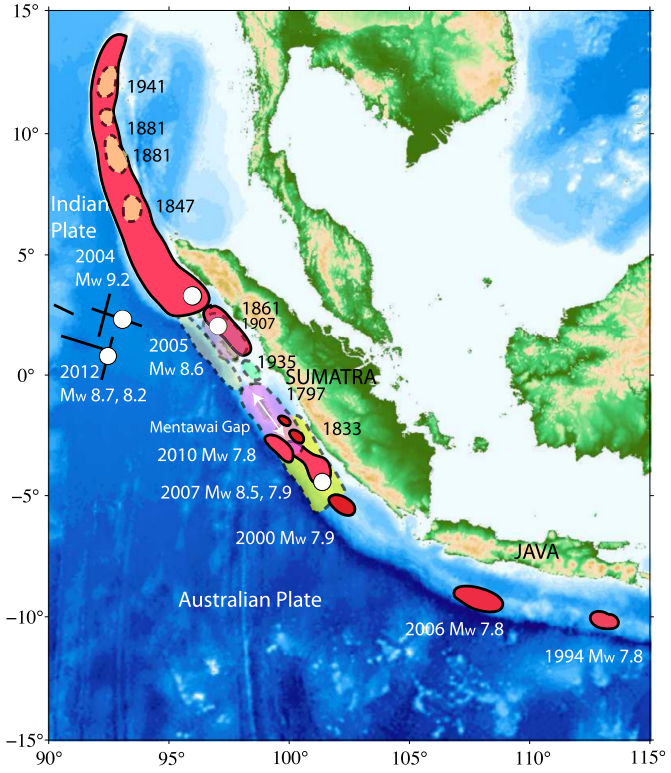

Fig. 3. Recent and historic large events along Sumatra and Java. The epicenters of 5 great earthquakes along Sumatra are indicated by white dots. Recent interplate thrust faulting events discussed in the text have their rupture areas highlighted in red with black outlines. Historical large ruptures have rupture zones with pastel colors with dashed outlines. The system of strike-slip faults activated in the pair of great earthquakes in 2012 is indicated by black line segments.

there appears to be some persistent physical segmentation along the Sunda subduction zone delimiting great ruptures, such as between the 2004 and 2005 events (Meltzner et al., 2012), there also appears to have been significant overlap of historical ruptures along Sumatra elsewhere, as in 1797 and 1833 (e.g., Natawidjaja et al., 2006; Sieh et al., 2008). This complicates anticipation of future earthquake rupture dimensions, especially in the region of the great earthquake in 2007 and its large M_w 7.9 aftershock to the northwest (the two small rupture patches in Fig. 3) on the same day.

Nonetheless, the portion of the 1797 rupture zone from latitudes −0.5° to −3° that has not ruptured recently is identified as the Mentawai (or Padang) seismic gap (Fig. 3). This region is considered to have high potential for a future large earthquake, having been straddled by recent great interplate events (e.g., McCloskey et al., 2008). The region is a shaking and tsunami threat to the Mentawai Islands, the city of Padang, and surrounding coastal areas. With over two hundred years of plate motion since the last event, and clear geodetic evidence of interplate locking (Chlieh et al., 2008) southeastward from the Batu Islands to the Pagai Islands (along Siberut and Sipora Islands), there appears to be substantial accumulated moment deficit in the Mentawai gap, possibly comparable to that released in the 1833 event to the southeast.

While not a great earthquake, the M_w 7.8 Mentawai event of October 25, 2010 provided another surprise by rupturing the very shallow portion of the megathrust up-dip from the 2007 Sumatra earthquakes (Fig. 3). This event was a tsunami earthquake (e.g., Kanamori, 1972), with a very long rupture duration and strong tsunami excitation that resulted in 3–9 m runup and inundation

as far as 600 m inland on the Pagai Islands (e.g., Bilek et al., 2011; Lay et al., 2011b; Newman et al., 2011; Hill et al., 2012; Yue et al., 2014a). The Mentawai earthquake further demonstrated that the shallow toe of megathrusts up-dip of preceding large earthquakes on the central megathrust can fail in large tsunamigenic earthquakes, as had been indicated by previous tsunami events thought to occur in the shallow wedge along the Kuril Islands (e.g., Fukao, 1979; Pelayo and Wiens, 1992). This places greater importance on establishing the up-dip limit of slip during great megathrust ruptures for assessing ensuing seismic and tsunami hazards. The earthquake in 1907 located seaward of the great 2005 rupture appears to have been a tsunami earthquake as well (Kanamori et al., 2010), so such events may also occur before rupture of the central megathrust.

The 17 July 2006 M_w 7.8 Java tsunami earthquake located eastward along the Sunda subduction zone (Fig. 3) had similarly ruptured right to the trench, up-dip of what appears to be an aseismic central megathrust (e.g., Ammon et al., 2006). The June 2, 1994 M_w 7.8 event even further to the east also has tsunami earthquake characteristics, but may not have ruptured all the way to the trench (e.g., Abercrombie et al., 2001). It has often been assumed that the sedimentary wedge near the toe will have slip-strengthening friction and will deform aseismically rather than fracture (e.g., Byrne et al., 1988; Marone and Scholz, 1988), but the 2006 Java and 2010 Mentawai events indicate that the seismic hazard of near-trench thrusting has generally been underestimated. The comparable-size October 28, 2012 M_w 7.8 Haida Gwaii thrust earthquake offshore of western Canada involved slip entirely localized beneath a sedimentary wedge seaward of the Queen Charlotte fault (Lay et al., 2013b), demonstrating that even undeveloped subduction zones can experience very shallow tsunamigenic faulting under sediments.

It is not unusual for great interplate ruptures to induce intraplate faulting below the trench and outer rise, typically involving normal faulting with a near-horizontal tension axis aligned in the subducting plate motion direction (e.g., Christensen and Ruff, 1988; Lay et al., 1989), but the April 11, 2012 M_w 8.7 and 8.2 strike-slip earthquakes that ruptured several hundred kilometers seaward of the 2004 M_w 9.2 rupture zone were unprecedented. These events ruptured a network of at least 5 conjugate or orthogonal fault segments (Fig. 3) spread over hundreds of kilometers (e.g., Meng et al., 2012; Yue et al., 2012; Wei et al., 2013a). It appears that stress transfer from the 2004 underthrusting event influenced the timing of the ruptures (e.g., Delescluse et al., 2012), but their overall faulting represents lithospheric-wide deformation along a nascent plate boundary between the increasingly independent Indian and Australian plates. The 2012 mainshock is both the largest strike-slip faulting event and the largest intraplate earthquake that has been seismologically recorded. New fault segments appear to have been activated and the network of faults that ruptured could not have been anticipated based on seismic history or tectonic structures.

Kuril Islands

Two great earthquakes that struck along the central Kuril Island arc on November 15, 2006 (M_w 8.4) and January 13, 2007 (M_w 8.1) represent the more typical interaction between the interplate and intraplate trench slope environment, but still offered several surprises. In this case, the first event was a large interplate thrust earthquake at shallow depth on the megathrust within a region that had uncertain seismic potential due to lack of recorded historical earthquakes and distinct characteristics of the upper plate (including disruption of the volcanic arc, presence of an unusual large forearc basin, and narrowing of the trench). The event likely ruptured to the trench, and immediately induced

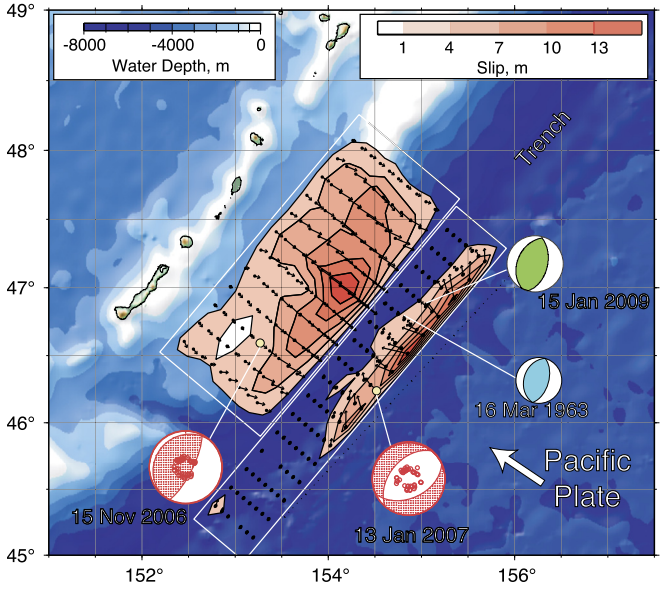

Fig. 4. Surface map projection of co-seismic slip for the 15 November 2006 (average slip 7.0 m) and the northwest dipping plane for 13 January 2007 (average slip 6.7 m at depths less than 25 km) events (NEIC epicenters: yellow circles). GCMT mechanisms with P-wave sampling for the doublet events are shown in red. The focal mechanism and epicenter of the 16 March 1963 (blue mechanism) and 15 January 2009 (green mechanism) compressional trench-slope events (hexagons) are included. The arrow indicates the direction of the Pacific plate motion relative to the Okhotsk plate at 80 mm/yr. Modified from Lay et al. (2009).

normal-faulting aftershock activity in the outer trench slope region of the Pacific plate that included a second great event within two months (Fig. 4) (Ammon et al., 2008; Steblov et al., 2008; Lay et al., 2009; Raeesi and Atakan, 2009). This second event was much larger than typical intraplate activity induced by large thrust events (Christensen and Ruff, 1988), and the pair of events is called a doublet to emphasize the triggering interaction between the comparable-size events.

This was the first documented great earthquake doublet to involve both thrust and normal faulting. Concentration of slip at very shallow depth on the megathrust during the first event may have allowed total stress drop that enhanced the increment of extensional stress manifested in the great normal-faulting event. The large thrust was preceded by a relatively deep trench slope compressional event on March 16, 1963 (M_S 7.2) (Christensen and Ruff, 1988), and followed by another on January 15, 2009 (M_w 7.4) (Fig. 4), indicating temporal modulation of the slab bending stress environment by the interplate earthquake strain accumulation and release.

Solomon Islands

The central Solomon Islands megathrust had an uncertain seismic potential like that for the central Kuril region due to lack of historical interplate seismicity and complex structure, in this case involving the subducting lithosphere. A ridge/transform boundary intersects the subduction zone, producing a triple junction, with the Solomon Sea plate subducting on the northwestern side of the boundary and the Australian plate subducting on the southeastern side (Fig. 5). It is often inferred that interplate coupling is affected by subduction of strong bathymetric features, and given the very young, warm oceanic lithosphere entering the trench in this region with slight divergence between the plates subducting on either side, it seemed unlikely for a great earthquake to strike this region. On April 1, 2007, this line of reasoning was proved wrong by an M_w 8.1 interplate earthquake rupturing at

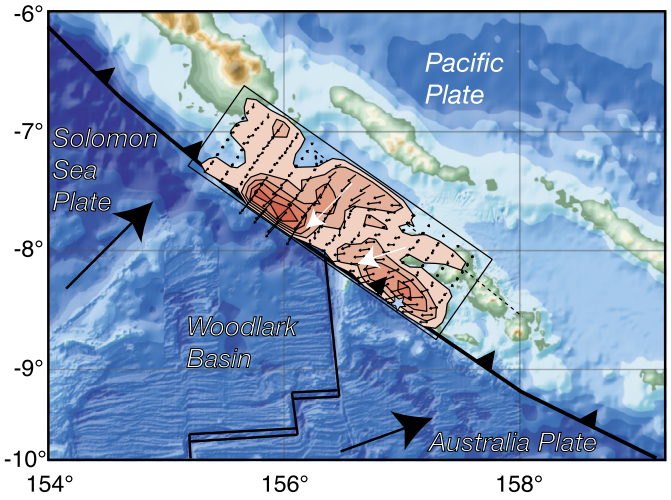

Fig. 5. Slip distribution over the model grid for the April 1, 2007 Solomon Islands (M_w 8.1) earthquake obtained from inversion of teleseismic body wave observations. The blue star indicates the epicenter. The plate tectonic setting is defined by two plates, the Solomon Sea plate and Australia plate subducting with slightly different relative motions beneath the Pacific plate. The black arrows indicate the plate motion directions relative to a fixed Pacific plate. The peak slip in the model is 6.6 m, with the slip distribution being contoured with 1 m slip intervals. Directions of co-seismic slip of the Pacific plate are indicated by the small black arrows. These differ in the two slip patches, and correspond to the relative motion between the plates on either side of the triple junction as indicated the large white arrows. Modified from Furlong et al. (2009).

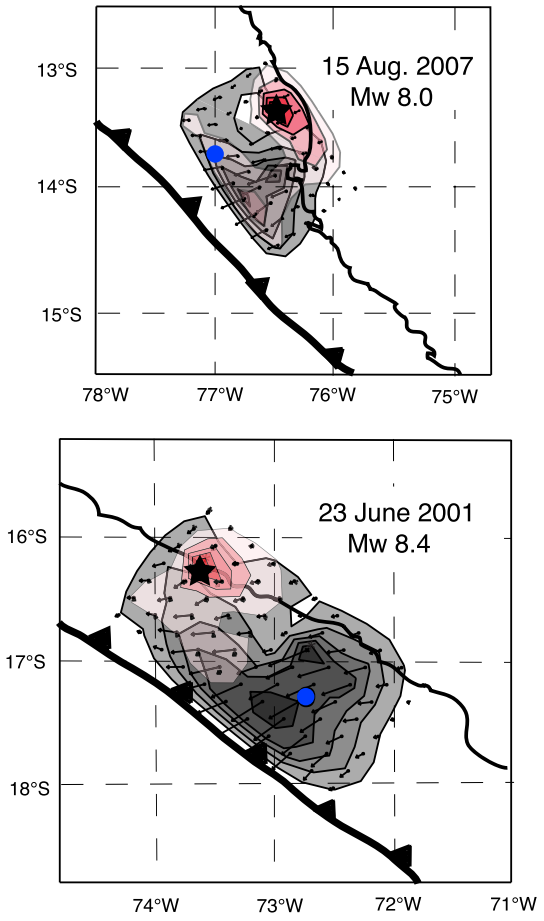

Fig. 6. Maps showing the slip distribution for the compound event models for the 2007 (top) and 2001 (bottom) Peru earthquakes. The black stars indicate the event epicenters. The blue dots are the CMT centroid locations. The slip region for the first event in each pair is indicated by the red tones. The slip vectors are shown by the black vectors over the source grid, with slip being contoured. Peak slip for the 2007 event is 10.6 m, with the initial event having peak slip of 3.8 m. Peak slip for the 2001 event is 97 m, with the initial event having peak slip of 2.5 m. From Lay et al. (2010a).

shallow depth on the megathrust with slip extending right across the triple junction (e.g., Taylor et al., 2008; Furlong et al., 2009; Chen et al., 2009). Furlong et al. (2009) found two concentrations of large slip on either side of the triple junction by seismic inversion (Fig. 5), and remarkably, the direction of slip in each patch corresponds to the distinct relative motion directions between the subducting plates and the overriding Pacific plate. Essentially, the two plates underthrust at the same time in slightly different directions. The peak tsunami runup was 12 m, and coral uplift and subsidence data support the strong tsunamigenesis being the result of near-trench slip (Chen et al., 2009).

Very shallow rupture to the trench also occurred during the February 6, 2013 Santa Cruz Islands M_w 8.0 rupture in the easternmost Solomon Islands at the northern end of the Vanuatu arc (Fig. 1). A two slip patch rupture occurred with the first patch being deeper on the megathrust and the second occurring along strike and up-dip, probably rupturing to the trench and accounting for large tsunami generated by the event (Lay et al., 2013a). This event occurred in a seismic gap with no known prior thrusting rupture, and a remarkably complex foreshock and aftershock sequences accompanied the rupture, with a possibility of triggered slow slip of the adjacent megathrust region (Hayes et al., 2014a).

Peru

During the decade long surge of great earthquakes, one thrust event struck offshore of Peru on August 15, 2007 (M_w 8.0) (Fig. 1). This event struck near Pisco, and produced substantial shaking damage and a tsunami on the Paracas peninsula. The seismic, geodetic and tsunami data for this event has been well studied (e.g., Pritchard et al., 2007; Motagh et al., 2008; Pritchard and Fielding, 2008; Biggs et al., 2009; Lay et al., 2010a; Sladen et al., 2010), and the event is not surprising in location, size, or geometry of faulting. However, the rupture involved two slip episodes, with about 60 s between the subevents. It appears that an initial, M_w 7.8 event occurred deep on the megathrust and its static and dynamic stresses triggered a nearby M_w 8.0 rupture (Fig. 6) (Lay et al., 2010a; Sladen et al., 2010). This type of compound rupture presents great challenges to early warning procedures that attempt to characterize imminent seismic and tsunami hazards from early energy release or ground deformation.

Lay et al. (2010a) further analyzed the June 23, 2001 Peru M_w 8.4 earthquake southeast of the Pisco event. They infer compound faulting in that case as well, with an initial M_w 7.5 event occurring on the deeper portion of the megathrust, with the Rayleigh waves triggering a much larger rupture that nucleated about 150 km away. The second rupture expanded bilaterally (Fig. 6); leading to an apparent reversal of rupture direction and possible re-rupture of the fault surface to the northwest (e.g., Robinson et al., 2006). While resolving whether any slip occurred during the time between the doublet subevents for these two Peru earthquakes is very difficult (Bilek and Ruff, 2002; Pritchard et al., 2007; Lay et al., 2010a; Sladen et al., 2010), they certainly involve a staggered cascade of slip that would usually be more concentrated in time during a typical great earthquake rupture.

Samoa/Tonga

Three great earthquakes struck along the Tonga subduction zone during the recent surge (Fig. 1), constituting some of the

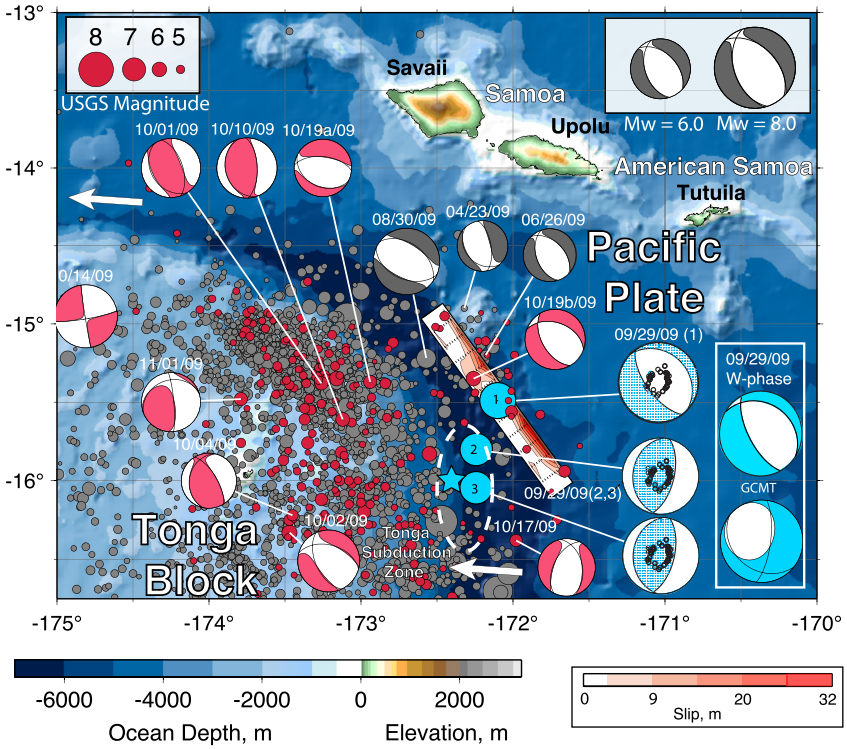

Fig. 7. The great (M_w 8.1) September 29, 2009 Samoa earthquake ruptured an outer trench-slope normal fault (#1 blue mechanism and numbered blue circle) and co-seismically triggered two initially unrecognized major (M_w 7.8, 7.8) thrust fault earthquakes (#2,3 blue mechanisms and circles) that together comprise an M_w 8.0 thrust event on the megathrust. Distribution of teleseismic P waves used in the finite-source inversion are indicated by the black circles in the blue mechanisms. The star indicates the centroid location estimated for event 3 from regional surface wave modeling. In this region the Pacific plate approaches the Tonga subduction zone, tears, and the southern part thrusts down under the Australian Plate. The locations and magnitudes of three moderate-size ($M_W = 5$ to 6.6) trench-wall/outer-rise extensional events between April and August 2009 for which GCMT solutions (gray coloring) are indicated. Red circles indicate epicenters and magnitudes for the mainshock and aftershocks, most of which are not on the mainshock rupture plane. Preceding regional seismicity is shown by the gray circles. The W-phase and GCMT point-source solutions (inset blue mechanisms) for the mainshock and GCMT solutions for the larger aftershocks (red coloring) are shown. The large arrows indicate the direction and rate of motion of the Pacific Plate relative to the Australian plate (from the global plate motion model NUVEL-1). Major islands of Samoa and American Samoa are indicated. From Lay et al. (2010c).

largest events to have been recorded in the region. However, none of them were conventional interplate thrusts. The May 3, 2006 M_w 8.0 thrust event in central Tonga has a centroid depth of 65 km, and while the mechanism is similar to an interplate rupture, the event occurred within the subducting Pacific plate. On September 29, 2009 an M_w 8.1 event struck near the northern end of the Tonga arc, located under the outer trench slope. The overall source mechanism from long-period analyses is normal faulting (Fig. 7), and finite-fault inversion indicates the initial rupture involved large slip at shallow depth extending along a 150 km long fault (Lay et al., 2010c), similar to the January 13, 2007 M_w 8.1 Kuril trench-slope earthquake mentioned above. However, the aftershock sequence was widely distributed on or above the megathrust to the west (Fig. 7), and the inconsistency of the long-period W-phase and GCMT solutions for the event indicated complexity of the rupture. Detailed analysis of regional and teleseismic data resolved two thrust-faulting subevents during a two-minute-long rupture process, located on the megathrust about 50 km south of the normal faulting. The total seismic moment of the two subevents is equal to that of an M_w 8.0 thrust event. This triggered thrust event was also detected by eastward offset of a GPS station in the Tonga arc (Beavan et al., 2010).

The 2009 Samoa earthquake thus involved a surprising example of a great normal-faulting earthquake triggering a great thrust-faulting earthquake, inverting the typical interaction between interplate and intraplate environments. While not identified as a separate event in the standard earthquake catalogs, we count this triggered thrust event among the surge of great earthquakes because it is the largest recorded event known to involve interplate thrusting along the Tonga arc, making it important for seismic hazard assessments. The underthrusting rupture appears to have been concentrated at shallow depth, and the wide activation of thrust-faulting aftershock activity may represent triggering of small events over a weakly-coupled megathrust zone. The interference of seismic radiation from the overlapping normal and thrust faulting was difficult to interpret, and if such complex pairs of triggered events with very different mechanisms have occurred in the past century, only the initial event may have been recognized. Nonetheless, it seems likely that this was a very rare type of great earthquake doublet given the rarity of finding major inconsistency of long-period moment tensor determinations and such widespread aftershock patterns with different mechanisms from the mainshock.

Chile

Two great earthquakes struck in well-recognized seismic gaps along Chile during the surge (Fig. 1), but both offered surprises in their rupture extent. The February 27, 2010 Maule (M_w 8.8) earthquake ruptured the plate boundary offshore of central Chile between 34°S and 38.5°S (Fig. 8b). Slip in this event has been determined by analysis of seismic, geodetic, and tsunami observations (e.g., Delouis et al., 2010; Lay et al., 2010b; Tong et al., 2010; Pollitz et al., 2011b; Vigny et al., 2011; Moreno et al., 2012; Lin et al., 2013; Yue et al., 2014b). Two large slip regions are resolved along the megathrust, one extending from 34°S to 35°S and the other from 37°S to 38°S. Yue et al. (2014b) find that the large-slip in these patches likely extends all the way to the trench, and there were concentrations of trench-slope normal faulting

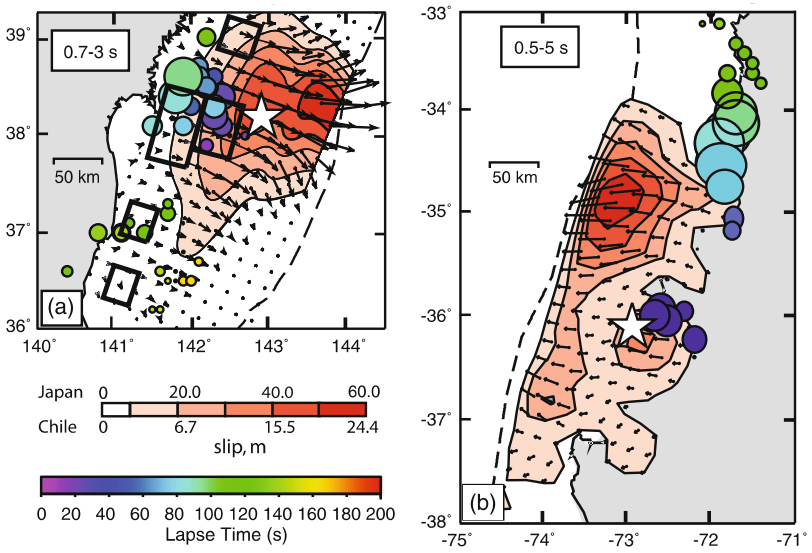

Fig. 8. Maps summarizing rupture characteristics for (a) the 11 March 2011 Tohoku, Japan (M_w 9.0) and (b) the 27 February 2010 Maule, Chile (M_w 8.8) earthquakes. The white stars indicate the epicentral locations used for each rupture model. The co-seismic slip distributions are those determined from teleseismic body wave recordings for the Tohoku event by Lay et al. (2011a) and for the Chile event by Koper et al. (2012). The vectors indicate the variable slip direction for subfaults, with the contoured color scale indicating the total slip at each position. The position and timing of sources of coherent short-period teleseismic P wave radiation in the bandpass indicated in each panel imaged by back-projection of recordings at North American seismic stations, mainly from the EarthScope Transportable Array, are shown by the colored circles, with radius scaled proportional to relative beam power (from Koper et al., 2011a, 2011b for Tohoku, and Koper et al., 2012 for Chile). The rectangles in (a) indicate estimated source locations of high frequency strong ground motions determined by Kurahashi and Irikura (2011). Note that the regions with large slip locate up-dip, toward the trench (dashed line) in each case, whereas the coherent short-period radiation is from down-dip, near the coastline. From Lay et al. (2012).

in the along-plate motion direction offshore from these patches. The most surprising aspect of this slip distribution is that the region in between the patches, in the inferred source area of the historic 1835 rupture that was the primary basis for defining the seismic gap, the co-seismic slip was minor. The northern slip patch overlapped relatively recent rupture zones from 1928 and 1985 earthquakes, and the southern slip patch overlapped the northern end of the 1960 rupture zone (Lay, 2011; Lorito et al., 2011).

The April 1, 2014 M_w 8.1 Iquique, Chile earthquake ruptured the northern Chile megathrust from 19.5°S to 20.5°S, within the northern third of the large seismic gap along the great 1877 rupture zone (Hayes et al., 2014b; Lay et al., 2014; Ruiz et al., 2014; Schurr et al., 2014). The large-slip zone for the earthquake is unusually concentrated for a great earthquake, extending only about 70 km in length and 50 km in width. The rupture was preceded by months of slowly migrating foreshock activity located up-dip of the eventual mainshock, suggesting along-dip variation in frictional properties on the megathrust. The rupture of only a small fraction of the 1877 gap indicates that northern Chile does not fail with characteristic great earthquakes, but may behave like the megathrust along Ecuador–Colombia, where the great rupture zone of the 1906 M_w 8.8 earthquake re-ruptured in three smaller events in 1942 (M_S 7.9), 1958 (M_S 7.8) and 1979 (M_w 8.2) (Kanamori and McNally, 1982). The unbroken region of the 1877 gap in northern Chile remains a likely site for future great earthquake activity.

These two events demonstrate the value of historical earthquake activity and the seismic gap notion for anticipating the regions where future great events may occur, but also show the limitations of our seismological characterization of repeated rupture of each region with respect to anticipating how large the events will be and where slip will be concentrated.

Honshu

The April 11, 2011 Tohoku, Japan (M_w 9.0) earthquake (Fig. 1) produced a massive tsunami along Honshu by unexpectedly rupturing the entire width of the megathrust from below the coast to the trench (see reviews by Lay and Kanamori, 2011; Ritsema et al., 2012). The rupture spread over many smaller rupture zones of large events from 1936 to 2005 along the deeper portion of the megathrust, as well as shallower regions that had failed in 1897, 1915 and 869. A large-slip zone extended about 200 km along the subduction zone with average slip of about 25 m, but slip appears to have increased to 50–60 m near the toe of the wedge (Fig. 8a) (e.g., Yue and Lay, 2013; Hayes, 2011; Ide et al., 2011; Lay et al., 2011a; Lee, 2011; Shao et al., 2011; Yoshida et al., 2011; Yamazaki et al., 2011, 2013; Yue and Lay, 2011). The increased slip near the toe can account for the large tsunami excitation using elastic models (e.g., Fujii et al., 2011; Lay et al., 2011c; Maeda et al., 2011; Yokota et al., 2011; Satake et al., 2013), but the precise location and timing and possible anelastic contributions remain contested. In particular, some, but not all, inversions of static geodetic data and some seismic data tend to place peak slip further down-dip (e.g., Iinuma et al., 2011; Koketsu et al., 2011; Pollitz et al., 2011a; Simons et al., 2011). The event demonstrated the lack of strong segmentation along the Japan subduction zone and the potential for rare great earthquakes to enhance their overall slip distribution relative to smaller ruptures of the same megathrust, as was the case for the 1906 Ecuador–Colombia rupture. The Tohoku event also generated the most intensive activation of intraplate normal faulting over the outer trench slope and outer rise that has been observed, raising concerns about possible occurrence of a future great normal faulting rupture similar to the 1933 Sanriku-Oki event that struck north of the 2011 region (e.g., Lay et al., 2011d).

3. Great earthquake quantification

Many of the surprising attributes of the recent great earthquakes have only been revealed because of great advances in recording the ground motions and tsunamis that were generated. This has involved expanded global networks of digital seismic stations, extensive campaign and permanent GPS installations, deployment of dense regional networks in some regions, large increase in number of deep-water ocean bottom pressure sensors

of the DART buoy network, ocean bottom seismometer deployments, InSAR and LandSAT imaging, and GRACE and GOCE gravity field measurements, along with numerous other efforts. The hundreds of studies of the recent great earthquakes provide a panoply of applications of the new data sets to constrain processes before, during and after the events. All of the great ruptures of the past decade have been studied in detail, most by joint inversions or modeling of multiple data sets, such that the events are better characterized than was possible for any of the great events of the last century. Every earthquake is distinct, with a local tectonic context and specific failure processes, making it hard to distill general attributes quantitatively.

One aspect of the recent large megathrust failures that has been revealed by new data sets and data processing involves the co-seismic distribution of short-period energy release over the fault relative to the location of large slip (Fig. 8). Back-projection of teleseismic short-period P waves from great earthquakes to image space–time locations of coherent bursts of short-period energy was introduced for the 2004 Sumatra event by Ishii et al. (2005). Numerous applications have been made to recent great earthquakes and a variety of methodologies have been introduced for such imaging (e.g., Walker et al., 2005; Krüger and Ohrnberger, 2005; Ishii et al., 2007; Xu et al., 2009; Ishii, 2011; Koper et al., 2011a, 2011b, 2012; Meng et al., 2011; Yao et al., 2011; Wang and Mori, 2011a, 2011b; Zhang et al., 2011). Short-period seismic radiation is sensitive to slip accelerations and small-scale rupture variations, and the degree to which it can be deterministically imaged for large ruptures that have diffuse energy release from the slip zone is limited. However, consistent observations of spatial separation of zones of coherent short-period energy release from regions of large co-seismic slip were first well-documented for the March 11, 2011 Tohoku earthquake (Fig. 8a). While large slip extended to the trench, this appears to have occurred without releasing localized bursts of short-period seismic waves, whereas the down-dip region with relatively modest co-seismic slip released bursts of energy with 0.5–3 s period that could be imaged by several teleseismic back-projection methods. The local strong motion recordings from stations in Japan also enabled imaging of concentrations of higher frequency radiation that correspond well with the teleseismic back-projections of short-period P waves. Similar, along-dip separation of high-frequency radiation bursts relative to the shallower large-slip distribution for the 2010 Maule, Chile earthquake has also been established (Fig. 8b) (e.g., Kiser and Ishii, 2011; Koper et al., 2012). Lay et al. (2012) find that a similar tendency for coherent bursts of short-period radiation to locate deeper on the megathrust holds for several other recent great megathrust earthquakes.

One of the most important new developments of the past decade has been the accumulation of GPS deformation measurements along plate boundaries and analysis of upper plate strain accumulation. The 2010 Maule, Chile and 2011 Tohoku, Japan great earthquakes struck along coastlines where extensive GPS networks had accumulated up to two decades of preceding ground motions that could be modeled by slip-deficit distributions on the megathrust (e.g., Nishimura et al., 2004; Suwa et al., 2006; Hashimoto et al., 2009; Loveless and Meade, 2010; Moreno et al., 2010). While these measurements have limited sensitivity to coupling far offshore, and the slip-deficit models failed to anticipate the location of largest slip for the 2011 event, these studies demonstrated the potential for mapping out future large earthquake rupture zones. The 2014 Iquique, Chile earthquake further validated this potential, as the foreshock sequence occurred in a region imaged to have modest slip-deficit, while the main slip occurred in a strongly locked region (e.g., Métois et al., 2012; Béjar-Pizarro et al., 2013). Perhaps one of the most compelling demonstrations of the potential for precise imaging of megathrust slip-deficit regions to define future rupture zones is offered by the September 5, 2012 Nicoya, Costa Rica M_w 7.6 rupture, for which protrusion of the Nicoya peninsula seaward over the megathrust to within 60 km of the trench allowed GPS deployments to achieve good spatial resolution of a slip-deficit patch on the underlying megathrust (e.g., Feng et al., 2012). This patch very closely corresponds to the co-seismic rupture zone in 2012, which is equally well resolved due to the distribution of overlying seismic and geodetic instrumentation (Yue et al., 2013). Achieving comparable resolution for future megathrust events located offshore will require expansion of seafloor geodesy.

Recordings of high sample rate GPS positions have greatly increased in many regions, and the resulting time series have proved very valuable in inversions for slip distributions of recent great earthquakes (e.g., Ammon et al., 2011; Yue and Lay, 2011, 2013; Yue et al., 2013, 2014a, 2014b). Wider deployment of such stations to cover poorly instrumented subduction zones will improve resolution of slip in future events. While very short-period signals are not well resolved, the complete recovery of long-period seismic motions and their evolution into static offsets augments standard geodetic inversions by adding time-sensitive information that can reduce the slip versus distance trade-off of most offshore inversions (e.g., Yue and Lay, 2013).

The 2005 Sumatra, 2011 Japan and 2010 and 2014 Chile earthquakes also have excellent geodetic and seismic constraints on afterslip (e.g., Hsu et al., 2006; Ozawa et al., 2011) and aftershock sequence evolution due to availability of nearby permanent or temporary instrument networks. Massive aftershock sequences in Japan and Chile have been recorded and analyzed for their relationship to post-seismic deformation, stress transfer, and frictional variations. Each region appears to have unique attributes that will not be described here, but a systematic consideration of the distribution of larger interplate aftershocks relative to the large-slip regions imaged for all of the recent great earthquakes indicates a tendency for shallow slip regions to have few interplate aftershocks, whereas deeper regions have intermingled slip and aftershocks (Meng, Lay, and Kanamori, in preparation).

4. Discussion and conclusions

This overview of the great earthquake activity of the last decade is intended to convey the diversity of such events and their surprising revelations about faulting interactions, location of faulting, and associated shaking and tsunami hazards. Fig. 9 schematically captures aspects of the diversity of recent great ruptures, involving scenarios with (A) along-strike activation of adjacent great events as occurred in the 2004–2005 Sumatra events; (B) rupture across bathymetric and lithospheric discontinuities as occurred in the 2007 Solomon Islands event; (C) occurrence of shallow tsunami earthquakes up-dip of deeper great megathrust ruptures as occurred for the 2007 Sumatra and 2010 Mentawai ruptures; (D) co-seismic rupture to the trench as occurred on massive scale for 2011 Tohoku and in patches for 2010 Maule, Chile, and (E) triggering interactions between interplate and intraslab events or (F) vice-versa, as occurred in the 2006–2007 Kuril and 2009 Samoa doublets, respectively. The compound ruptures of the 2001 and 2007 Peru events add to the complexity of shallow subduction zone great earthquake phenomena. The intraplate April 11, 2012 Indo–Australian strike slip sequence and December 23, 2004 Macquarie M_w 8.1 strike-slip event (Fig. 1) (Hayes et al., 2009; Robinson, 2011; Kennett et al., 2014) represent great ruptures within oceanic lithosphere in regions of complex deformation that lack clear kinematic budgets to guide assessment of their occurrence or future event potential. The May 24, 2013 deep focus Sea of Okhotsk rupture (Fig. 1) is the largest (M_w 8.3), longest rupture length, and longest duration deep earthquake that has

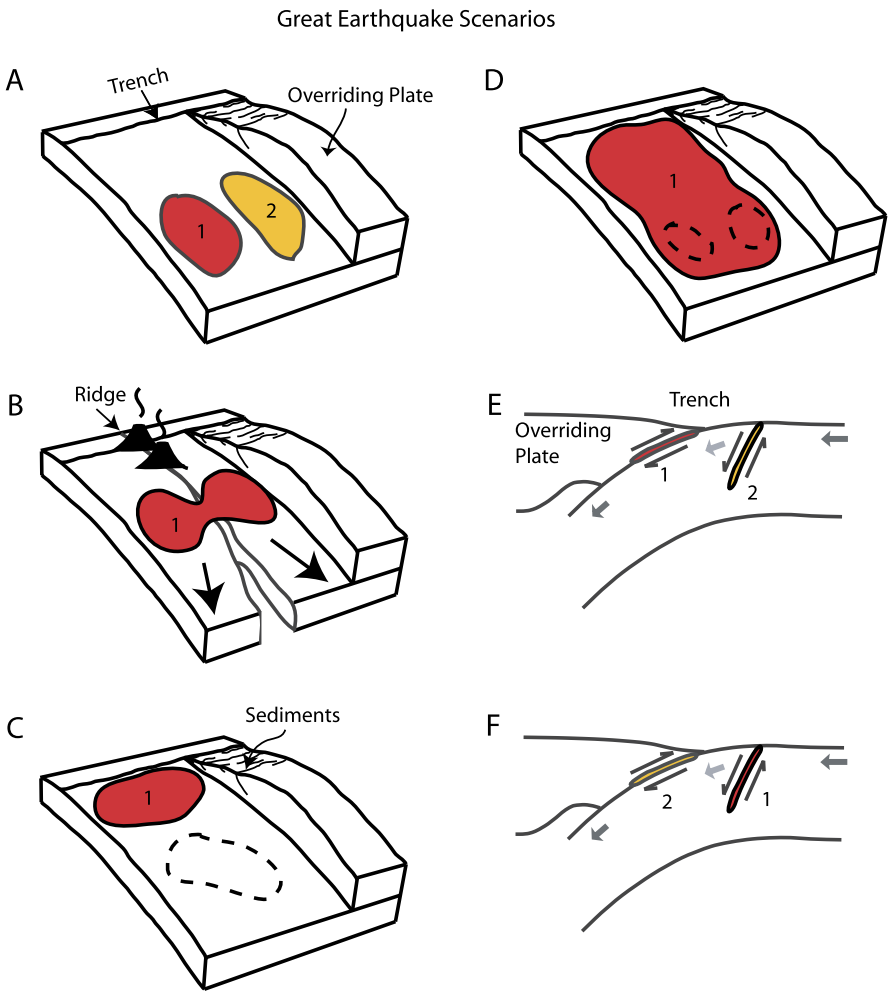

Fig. 9. Schematic scenarios of recent great (and very large) earthquake ruptures and triggering interactions discussed in the text.

been recorded (e.g., Ye et al., 2013c; Wei et al., 2013b), and its major differences from the 1994 Bolivia (M_W 8.3) demonstrate that diversity of deep great earthquake occurrence is comparable to that for shallow events.

Given the unique context of each great event in the recent surge, there is no unifying characterization that provides insight into the full ensemble. Stress transfer and triggering interactions are clearly demonstrated by several of the doublet sequences and the complexity of faulting of many of the events; but there are major challenges in quantifying associated risks. For example, the 2011 Tohoku event produced extensive normal faulting in the seaward Pacific plate, with more than 1000 moderate size events, but as yet, no great rupture comparable to the 1933 Sanriku-oki event has occurred. The smaller 2006 Kuril event also ruptured at shallow depth, but did produce a great trench-slope event. It is not clear what controls the different intraplate responses to the interplate failures. Many regions up-dip of large thrust events that appear not to have ruptured to the trench have not experienced shallow tsunami earthquakes; how can we assess whether they will or whether aseismic deformation will accommodate plate motion? Many such open-ended questions arise, and while the recent events have broadened our perspective of potential complexity, key issues remain unresolved.

Focusing on megathrust environments, where the majority of the recent great earthquakes have occurred, does offer some opportunity to synthesize the observations in terms of depth-varying rupture attributes and general spatial heterogeneity characteristics. Schematics are presented in Fig. 10, focusing on the along-dip variation of short-period energy release documented by Lay et al. (2012), who introduced depth-varying domains with distinct seismic radiation characteristics. This builds on earlier investigations of depth-dependent rupture characteristics of smaller events (e.g., Bilek and Lay, 1998, 1999, 2002; Bilek, 2007; Lay and Bilek, 2007). There is very little short-period seismic radiation but strong tsunami excitation from the shallowest domain A where tsunami earthquakes occur, modest levels of diffuse short-period radiation and large slip from the central domain B where most megathrust events occur, and concentrated bursts of short-period radiation during domain C events at depths of 30–50 km that accentuate strong ground shaking hazard from the deeper ruptures. Domain D represents a transition at the deep edge of the seismogenic zone, only present in some regions, with diverse observations of slow slip events, low-frequency earthquakes, and/or seismic tremor. The 2D schematic of variable frictional or slip properties in Fig. 10 emphasizes that these variations likely arise from spatial heterogeneity in frictional properties rather than simple pressure-dependence of friction. Similar characterization of fault zone structures has been suggested by Uchida and Matsuzawa (2011). Efforts to image structural features in the environment that may control the scale lengths of heterogeneity are still in early stages (e.g., Zhao et al., 2011).

These conceptual models of depth-varying seismic radiation properties have been tested using teleseismic and regional spectral methods applied to events in individual subduction zones along the Japan trench offshore of Honshu (Ye et al., 2013a) and along the Middle American trench (Ye et al., 2013b), yielding general

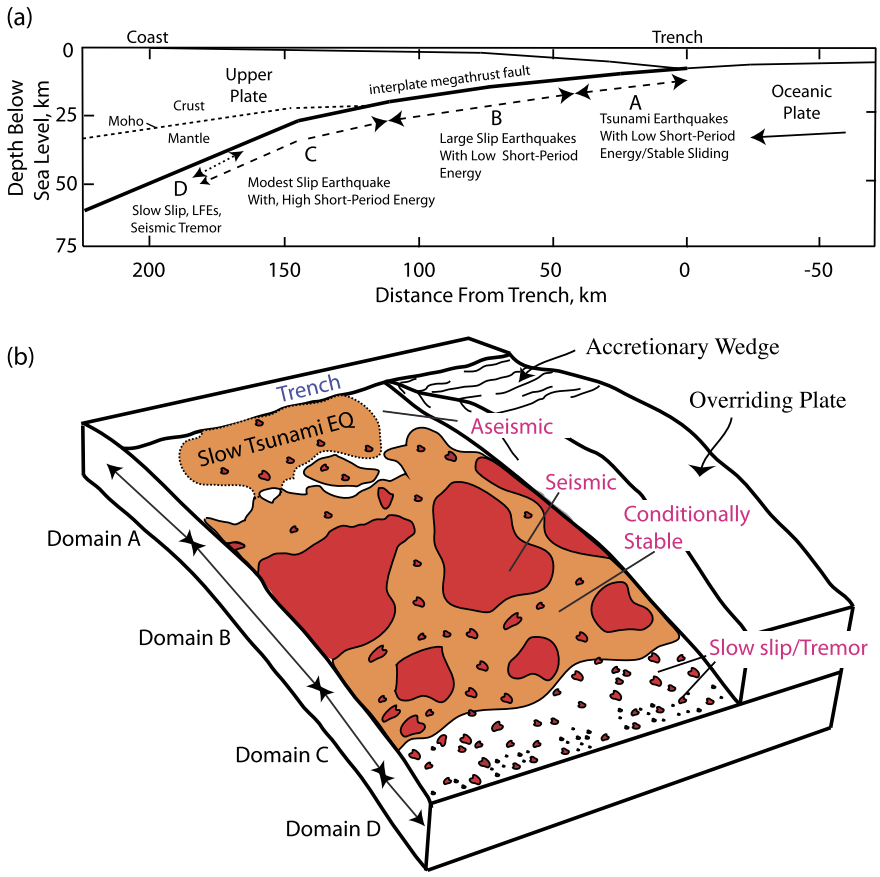

Fig. 10. (a) Schematic cross-section, scaled appropriately for the subduction zone off the northeast coast of Honshu where the great 2011 Tohoku earthquake occurred, indicating four domains of megathrust rupture characteristics: A – near-trench domain where tsunami earthquakes or anelastic deformation and stable sliding occur; B – central megathrust domain where large slip occurs with minor short-period seismic radiation; C – down-dip domain where moderate slip occurs with significant coherent short-period seismic radiation; D – transitional domain, only present in some areas, typically with a young subducting plate, where slow slip events, low frequency earthquakes (LFEs), and seismic tremor can occur. At yet greater depths the megathrust slides stably or with episodic slow slip or plastic deformation that does not generate earthquakes. (b) Cut-away schematic characterization of the megathrust frictional environment, related to Domains A, B, C and D defined in (a). Regions of unstable frictional sliding are red regions labeled "seismic". Regions of aseismic stable or episodic sliding are white regions labeled "aseismic". Orange areas are conditional stability (Scholz, 1998) regions, which displace aseismically except when accelerated by failure of adjacent seismic patches. Domain A is at shallow depth where sediments and pore fluids cause very slow rupture expansion even if large displacements occur in tsunami earthquakes. Domain B has large, relatively uniform regions of stable sliding that can have large slip, but generate modest amounts of short-period radiation upon failure. Domain C has patchy, smaller scale regions of stable sliding surrounded by conditionally stable areas. When these areas fail, coherent short-period radiation is produced. Small, isolated patches may behave as repeaters when quasi-static sliding of surrounding regions regularly load them to failure. Domain D is dominated by aseismic sliding, but many small unstable patches can rupture in seismic tremor when slow slip events occur. Modified from Lay et al. (2012).

support for depth-dependence of some aspects of megathrust ruptures. Isolation of the source spectra for magnitude 6.0–7.6 events off-shore Honshu with an empirical Green's function (EGF) method for regional network observations in Japan demonstrated that both depth-varying source radiation and path attenuation variations account for observed ground shaking patterns (Ye et al., 2013a). Further examination of rupture processes of all sizes is needed to advance the models beyond their current schematic nature.

There have been some observations of precursory slow slip events and migration of foreshock activity toward the site of mainshock initiation, notably for the 2011 Tohoku, Japan and 2014 Iquique, Chile earthquakes (see a discussion by Brodsky and Lay, 2014). The increasingly widespread availability of regional geodetic and seismic networks is capturing these processes for the first-time, and may offer some prospect of improved earthquake forecasting. Understanding the relationship of such processes to the heterogeneous frictional regime depicted in Fig. 10 is an important line of inquiry for the future.

The surge of great earthquakes from 2004–2014 has provided many demonstrations of the complexity of large earthquake ruptures and their interactions. Extensive seismic, geodetic and tsunami observations acquired for all of the events allow us to constrain the slip distributions and energy release far better than for prior great earthquakes, and newly discovered features such as depth-dependence of short-period energy release may lead to new understanding of how megathrust properties vary. The distribution of events in Fig. 1 indicates that more great events could strike in many locations, but the Mentawai and northern Chile gaps have clear potential. The western U.S. margin appears to hold potential as well, either along Cascadia or on the San Andreas system. The Himalayan thrust front is perhaps the continental region holding the most potential for a great earthquake outside the circum-Pacific. Looking forward, it is clear that offshore observations will be critical to resolving strain accumulation prior to great ruptures and sustained operation of dense networks of seismic, geodetic, and tsunami sensors is essential to making sufficient observations of complex earthquake faulting so that one day we will hopefully find fewer surprises attending every giant earthquake.

Acknowledgements

This work made use of GMT and SAC software. Reviews by an anonymous reviewer and Doug Wiens helped to improve the text. The IRIS DMS data center was used to access the seismic data from

Global seismic network and Federation of Digital Seismic Network stations. This work was supported by NSF grant EAR1245717.

References

Abercrombie, R.E., Antolik, M., Felzer, K., Ekström, G., 2001. The 1994 Java tsunami earthquake: slip over a subducting seamount. J. Geophys. Res. 106, 6595–6607. http://dx.doi.org/10.1029/2000JB900403.

Allen, T.I., Marano, K.D., Earle, P.S., Wald, D.J., 2009. PAGER-CAT: a composite earthquake catalog for calibrating global fatality models. Seismol. Res. Lett. 80 (1), 57–62. http://dx.doi.org/10.1785/gssrl.80.1.57.

Ammon, C.J., Ji, C., Thio, H.-K., Robinson, D., Ni, S., Hjorleifsdottir, V., Kanamori, H., Lay, T., Das, S., Helmberger, D., Ichinose, G., Polet, J., Wald, D., 2005. Rupture process of the great 2004 Sumatra–Andaman earthquake. Science 308, 1133–1139.

Ammon, C.J., Kanamori, H., Lay, T., Velasco, A.A., 2006. The 17 July 2006 Java tsunami earthquake. Geophys. Res. Lett. 33, L24308. http://dx.doi.org/10.1029/2006GL028005.

Ammon, C.J., Kanamori, H., Lay, T., 2008. A great earthquake doublet and seismic stress transfer cycles in the Central Kuril Islands. Nature 451, 561–565.

Ammon, C.J., Lay, T., Simpson, D.W., 2010. Great earthquakes and global seismic networks. Seismol. Res. Lett. 81, 965–971.

Ammon, C.J., Lay, T., Kanamori, H., Cleveland, M., 2011. A rupture model of the 2011 off the Pacific coast of Tohoku Earthquake. Earth Planets Space 63, 693–696. http://dx.doi.org/10.5047/eps.2011.05.015.

Banerjee, P., Pollitz, F., Nagarajan, B., Bürgmann, R., 2007. Coseismic slip distributions of the 26 December 2004 Sumatra–Andaman and 28 March 2005 Nias earthquakes from GPS static offsets. Bull. Seismol. Soc. Am. 97, S86–S102.

Beavan, J., Wang, X., Holden, C., Wilson, K., Power, W., Prasetya, G., Bevis, M., Kautoke, R., 2010. Near-simultaneous great earthquakes at Tongan megathrust and outer rise in September 2009. Nature 466, 959–963.

Béjar-Pizarro, M., Socquet, A., Armijo, R., Carrizo, D., Genrich, J., Simons, M., 2013. Andean structural control on interseismic coupling in the North Chile subduction zone. Nat. Geosci. 6, 462–467. http://dx.doi.org/10.1038/NGEO1802.

Ben-Naim, E., Daub, E.G., Johnson, P.A., 2013. Recurrence statistics of great earthquakes. Geophys. Res. Lett. 40, 3021–3025. http://dx.doi.org/10.1002/grl.50605.

Biggs, J., Robinson, D.P., Dixon, T.H., 2009. The 2007 Pisco, Peru, earthquake (M8.0): seismology and geodesy. Geophys. J. Int. 176, 657–669.

Bilek, S.L., 2007. Using earthquake source durations along the Sumatra–Andaman subduction system to examine fault-zone variations. Bull. Seismol. Soc. Am. 97, S62–70.

Bilek, S.L., Lay, T., 1998. Variation of interplate fault zone properties with depth in the Japan subduction zone. Science 281, 1175–1178.

Bilek, S.L., Lay, T., 1999. Rigidity variations with depth along interplate megathrust faults in subduction zones. Nature 400, 443–446.

Bilek, S.L., Lay, T., 2002. Tsunami earthquakes: possibly widespread manifestations of frictional conditional stability. Geophys. Res. Lett. 29 (14). http://dx.doi.org/10.1029/2002GL015215.

Bilek, S.L., Ruff, L.J., 2002. Analysis of the 23 June 2001 $M_w = 8.4$ Peru underthrusting earthquake and its aftershocks. Geophys. Res. Lett. 29 (20), 1960. http://dx.doi.org/10.1029/2002GL015543.

Bilek, S.L., Engdahl, E.R., DeShon, H.R., El Hariri, M., 2011. The 25 October 2010 Sumatra tsunami earthquake: slip in a slow patch. Geophys. Res. Lett. 38, L14306. http://dx.doi.org/10.1029/2011GL047864.

Briggs, R.W., Sieh, K., Meltzner, A.J., Natawidjaja, D., Galetzka, J., Suwargadi, B., et al., 2006. Deformation and slip along the Sunda megathrust in the great 2005 Nias-Simeulue earthquake. Science 311, 1897–1901.

Brodsky, E.E., Lay, T., 2014. Recognizing foreshocks from the 1 April 2014 Chile earthquake. Science 344, 700–702. http://dx.doi.org/10.1126/science.1255202.

Bufe, C.G., Perkins, D.M., 2011. The 2011 Tohoku earthquake: resumption of temporal clustering of Earth's megaquakes. Seismol. Res. Lett. Abs. 82, 455.

Byrne, D.E., Sykes, L.R., Davis, D.M., 1988. Loci and maximum size of thrust earthquake and the mechanics of the shallow region of subduction zones. Tectonics 7, 833–857.

Chen, T., Newman, A.V., Feng, L., Fritz, H.M., 2009. Slip distribution from the 1 April 2007 Solomon Islands earthquake: a unique image of near-trench rupture. Geophys. Res. Lett. 36, L16307. http://dx.doi.org/10.1029/2009GL039496.

Chlieh, M., Avouac, J.-P., Hjorleifsdottir, V., Song, T.-R.A., Ji, C., Sieh, K., Sladen, A., Hebert, H., Prawirodirdjo, L., Bock, Y., Galetzka, J., 2007. Coseismic slip and afterslip of the great M_w 9.15 Sumatra–Andaman Earthquake of 2004. Bull. Seismol. Soc. Am. 97, S152–S173. http://dx.doi.org/10.1785/0120050631.

Chlieh, M., Avouac, J.P., Sieh, K., Natawidjaja, D.H., Galetzka, J., 2008. Heterogeneous coupling of the Sumatran megathrust constrained by geodetic and paleogeodetic measurements. J. Geophys. Res. 113 (B5), B05305. http://dx.doi.org/10.1029/2007JB004981.

Christensen, D.H., Ruff, L.J., 1988. Seismic coupling and outer-rise earthquakes. J. Geophys. Res. 93, 13421–13444. http://dx.doi.org/10.1029/JB093iB11p13421.

Daub, E.G., Ben-Naim, E., Guyer, R.A., Johnson, P.A., 2012. Are megaquakes clustered? Geophys. Res. Lett. 39, L06308. http://dx.doi.org/10.1029/2012GL051465.

Delescluse, M., Chamot-Rooke, N., Cattin, R., Fleitout, L., Trubienko, O., Vigny, C., 2012. April 2012 intra-oceanic seismicity off Sumatra boosted by the Banda-Aceh megathrust. Nature 490, 240–244. http://dx.doi.org/10.1038/nature11520.

Delouis, B., Nocquet, J.-M., Vallée, M., 2010. Slip distribution of the February 27, 2010 $M_w = 8.8$ Maule earthquake, central Chile from static and high-rate GPS, InSAR, and broadband teleseismic data. Geophys. Res. Lett. 37, L17305. http://dx.doi.org/10.1029/2010GL043899.

Feng, L., Newman, A.V., Protti, M., González, V., Jiang, Y., Dixon, T.H., 2012. Active deformation near the Nicoya Peninsula, northwestern Costa Rica, between 1996 and 2010: interseismic megathrust coupling. J. Geophys. Res. 117, B06407. http://dx.doi.org/10.1029/2012JB009230.

Fujii, Y., Satake, K., 2007. Tsunami source of the 2004 Sumatra–Andaman earthquake inferred from tide gauge and satellite data. Bull. Seismol. Soc. Am. 97, S192–S207. http://dx.doi.org/10.1785/0120050613.

Fujii, Y., Satake, K., Sakai, S., Shinohara, M., Kanazawa, T., 2011. Tsunami source of the 2011 off the Pacific coast of Tohoku, Japan earthquake. Earth Planets Space 63, 815–820. http://dx.doi.org/10.5047/eps.2011.06.010.

Fukao, Y., 1979. Tsunami earthquakes and subduction processes near deep-sea trenches. J. Geophys. Res. 84, 2303–2314.

Furlong, K., Lay, T., Ammon, C.J., 2009. A great earthquake rupture across a rapidly evolving three-plate boundary. Science 324, 226–229.

Gonzalez-Huizar, H., Velasco, A.A., Peng, Z., Castro, R.R., 2012. Remote triggered seismicity caused by the 2011, M9.0 Tohoku-Oki, Japan earthquake. Geophys. Res. Lett. 39, L10302. http://dx.doi.org/10.1029/2012GL051015.

Hashimoto, C., Noda, A., Sagiya, T., Matsu'ura, M., 2009. Interplate seismogenic zones along the Kuril-Japan trench inferred from GPS data inversion. Nat. Geosci. 2, 141–144. http://dx.doi.org/10.1038/ngeo421.

Hayes, G., 2011. Rapid source characterization of the 03-11-2011 M_w 9.0 off the Pacific Coast of Tohoku earthquake. Earth Planets Space 63, 529–534. http://dx.doi.org/10.5047/eps.2011.05.012.

Hayes, G.P., Furlong, K.P., Ammon, C.J., 2009. Intraplate deformation adjacent to the Macquarie Ridge south of New Zealand: the tectonic evolution of a complex plate boundary. Tectonophysics 463, 1–14.

Hayes, G.P., Furlong, K.P., Benz, H.M., Herman, M.W., 2014a. Triggered aseismic slip adjacent to the 6 February 2013 M_w 8.0 Santa Cruz Islands megathrust earthquake. Earth Planet. Sci. Lett. 388, 265–272.

Hayes, G.P., Herman, M.W., Barnhart, W.D., Furlong, K.P., Riquelme, S., Benz, H.M., Bergman, E., Barrientos, S., Earle, P.S., Samsonov, S., 2014b. Continuing megathrust earthquake potential in Chile after the 2014 Iquique earthquake. Nature. http://dx.doi.org/10.1038/nature13677.

Hill, E.M., et al., 2012. The 2010 M_w 7.8 Mentawai earthquake: very shallow source of a rare tsunami earthquake determined from tsunami field survey and near-field GPS data. J. Geophys. Res. 117 (B6), B06402. http://dx.doi.org/10.1029/2012JB009159.

Hsu, Y.-J., Simons, M., Avouac, J.-P., Galetzka, J., Sieh, K., Chlieh, M., Natawidjaja, D., Prawirodirdjo, L., Bock, Y., 2006. Frictional afterslip following the 2005 Nias-Simeulue earthquake, Sumatra. Science 312, 1921–1926.

Ide, S., Baltay, A., Beroza, G.C., 2011. Shallow dynamic overshoot and energetic deep rupture in the 2011 M_w 9.0 Tohoku-oki earthquake. Science 332, 1426–1429.

Iinuma, T., Ohzono, M., Ohta, Y., Miura, S., 2011. Coseismic slip distribution of the 2011 off the Pacific coast of Tohoku earthquake (M9.0) estimated based on GPS data – was the asperity in Miyagi-oki ruptured? Earth Planets Space 63, 643–648. http://dx.doi.org/10.5047/eps.2011.06.013.

Ishii, M., 2011. High-frequency rupture properties of the M_w 9.0 off the Pacific coast of Tohoku earthquake. Earth Planets Space 63, 609–614. http://dx.doi.org/10.5047/eps.2011.07.009.

Ishii, M., Shearer, P.M., Houston, H., Vidale, J.E., 2005. Extent, duration and speed of the 2004 Sumatra–Andaman earthquake imaged by the Hi-Net array. Nature 435, 933–936.

Ishii, M., Shearer, P.M., Houston, H., Vidale, J.E., 2007. Teleseismic P wave imaging of the 26 December 2004 Sumatra–Andaman and 28 March 2005 Sumatra earthquake ruptures using the Hi-net array. J. Geophys. Res. 112, B11307. http://dx.doi.org/10.1029/2006JB004700.

Kanamori, H., 1972. Mechanism of tsunami earthquakes. Phys. Earth Planet. Inter. 6, 246–259.

Kanamori, H., 1977. The energy release in great earthquakes. J. Geophys. Res. 82, 2981–2987.

Kanamori, K., McNally, K.C., 1982. Variable rupture mode of the subduction zone along the Ecuador–Colombia coast. Bull. Seismol. Soc. Am. 72, 1241–1253.

Kanamori, H., Rivera, L., Lee, W.H.K., 2010. Historical seismograms for unraveling a mysterious earthquake: the 1907 Sumatra earthquake. Geophys. J. Int. 183, 358–374.

Kennett, B.L.N., Gorbatov, A., Spiliopoulos, S., 2014. Tracking high-frequency seismic source evolution: 2004 M_w 8.1 Macquarie event. Geophys. Res. Lett. 41, 1187–1193. http://dx.doi.org/10.1002/2013GL058935.

Kiser, E., Ishii, M., 2011. The 2010 M_w 8.8 Chile earthquake: triggering on multiple segments and frequency dependent rupture behavior. Geophys. Res. Lett. 38, L07301. http://dx.doi.org/10.1029/2011GL047140.

Koketsu, K., Yokota, Y., Nishimura, N., Yagi, Y., Miyazaki, S., Satake, K., Fujii, Y., Miyake, H., Sakai, S., Yamanaka, Y., Okada, T., 2011. A unified source model for the 2011 Tohoku earthquake. Earth Planet. Sci. Lett. 310, 480–487. http://dx.doi.org/10.1016/j.epsl.2011.09.009.

Konca, A.O., Hjorleifsdottir, V., Song, T.-R.A., Avouac, J. -Ph, Helmberger, D.V., Ji, C., Sieh, K., Briggs, R., Meltzner, A., 2007. Rupture kinematics of the 2005 M_w 8.6 Nias-Simeulue earthquake from the joint inversion of seismic and geodetic data. Bull. Seismol. Soc. Am. 97, S307–S322.

Konca, A.O., Avouac, J.-P., Sladen, A., Meltzner, A.J., Sieh, K., Fang, P., Li, Z., Galetzka, J., Genrich, J., Chlieh, M., Natawidgaga, D.H., Bock, Y., Fielding, E.J., Ji, C., Helmberger, D.V., 2008. Partial rupture of a locked patch of the Sumatra megathrust during the 2007 earthquake sequence. Nature 456, 631–635. http://dx.doi.org/10.1038/nature07572.

Koper, K.D., Hutko, A.R., Lay, T., 2011a. Along-dip variation of teleseismic short-period radiation from the 11 March 2011 Tohoku Earthquake (M_w 9.0). Geophys. Res. Lett. 38, L21309. http://dx.doi.org/10.1029/2011GL049689.

Koper, K.D., Hutko, A.R., Lay, T., Ammon, C.J., Kanamori, H., 2011b. Frequency-dependent rupture process of the 2011 M_w 9.0 Tohoku Earthquake: comparison of short-period P wave back-projection images and broadband seismic rupture models. Earth Planets Space 63, 599–602. http://dx.doi.org/10.5047/eps.2011.05.026.

Koper, K.D., Hutko, A.R., Lay, T., Sufri, O., 2012. Imaging short-period seismic radiation from the 27 February 2010 Chile (M_w 8.8) earthquake by back-projection of *P*, *PP*, and *PKIKP* Waves. J. Geophys. Res. 117, B02308. http://dx.doi.org/10.1029/2011JB008576.

Krüger, F., Ohrnberger, M., 2005. Tracking the rupture of the $M_w = 9.3$ Sumatra earthquake over 1150 km at teleseismic distance. Nature 435, 937–939.

Kurahashi, S., Irikura, K., 2011. Source model for generating strong ground motions during the 2011 off the Pacific coast of Tohoku Earthquake. Earth Planets Space 63, 571–576. http://dx.doi.org/10.5047/eps.2011.06.044.

Lay, T., 2011. Earthquakes: a Chilean surprise. Nature 471 (7337), 174–175. http://dx.doi.org/10.1038/471174a.

Lay, T., Bilek, S., 2007. Anomalous earthquake ruptures at shallow depths on subduction zone megathrusts. In: Dixon, T.H., Moore, J.C. (Eds.), The Seismogenic Zone of Subduction Thrust Faults. Columbia University Press, New York, pp. 476–511.

Lay, T., Kanamori, H., 2011. Insights from the great 2011 Japan earthquake. Phys. Today, 33–39.

Lay, T., Astiz, L., Kanamoir, H., Christensen, D.H., 1989. Temporal variation of large intraplate earthquakes in coupled subduction zones. Phys. Earth Planet. Inter. 54, 258–312. http://dx.doi.org/10.1016/0031-9201(89)90247-1.

Lay, T., Kanamori, H., Ammon, C.J., Nettles, M., Ward, S.N., Aster, R., Beck, S.L., Bilek, S.L., Brudzinski, M.R., Butler, R., DeShon, H.R., Ekstrom, G., Satake, K., Sipkin, S., 2005. The great Sumatra–Andaman earthquake of 26 December 2004. Science 308, 1127–1133.

Lay, T., Kanamori, H., Ammon, C.J., Hutko, A.R., Furlong, K., Rivera, L., 2009. The 2006–2007 Kuril Islands great earthquake sequence. J. Geophys. Res. 114, B113208. http://dx.doi.org/10.1029/2008JB006280.

Lay, T., Ammon, C.J., Hutko, A.R., Kanamori, H., 2010a. Effects of kinematic constraints on teleseismic finite-source rupture inversions: Great Peruvian Earthquakes of 23 June 2001 and 15 August 2007. Bull. Seismol. Soc. Am. 100, 969–994.

Lay, T., Ammon, C.J., Kanamori, H., Koper, K.D., Sufri, O., Hutko, A.R., 2010b. Teleseismic inversion for rupture process of the 27 February 2010 Chile (M_w 8.8) earthquake. Geophys. Res. Lett. 37, L13301. http://dx.doi.org/10.1029/2010GL043379.

Lay, T., Ammon, C.J., Kanamori, H., Rivera, L., Koper, K.D., Hutko, A.R., 2010c. The 2009 Samoa–Tonga great earthquake triggered doublet. Nature 466, 964–968.

Lay, T., Ammon, C.J., Kanamori, H., Xue, L., Kim, M.J., 2011a. Possible large near-trench slip during the 2011 M_w 9.0 off the Pacific coast of Tohoku earthquake. Earth Planets Space 63, 687–692. http://dx.doi.org/10.5047/eps.2011.05.033.

Lay, T., Ammon, C.J., Kanamori, H., Yamazaki, Y., Cheung, K.F., Hutko, A., 2011b. The 25 October 2010 Mentawai tsunami earthquake (M_w 7.8) and the tsunami hazard presented by shallow megathrust ruptures. Geophys. Res. Lett. 38, L13301. http://dx.doi.org/10.1029/2010GL046552.

Lay, T., Yamazaki, Y., Ammon, C.J., Cheung, K.F., Kanamori, H., 2011c. The 2011 M_w 9.0 off the Pacific coast of Tohoku Earthquake: comparison of deep-water tsunami signals with finite-fault rupture model predictions. Earth Planets Space 63, 797–801. http://dx.doi.org/10.5047/eps.2011.05.030.

Lay, T., Ammon, C.J., Kanamori, H., Xue, L., Kim, M.J., 2011d. Possible large near-trench slip during the 2011 M_w 9.0 off the Pacific coast of Tohoku Earthquake. Earth Planets Space 63 (7), 687–692. http://dx.doi.org/10.5047/eps.2011.05.033.

Lay, T., Kanamori, H., Ammon, C.J., Koper, K.D., Hutko, A.R., Ye, L., Yue, H., Rushing, T.M., 2012. Depth-varying rupture properties of subduction zone megathrust faults. J. Geophys. Res. 117, B04311. http://dx.doi.org/10.1029/2011JB009133.

Lay, T., Ye, L., Kanamori, H., Yamazaki, Y., Cheung, K.F., Ammon, C.J., 2013a. The February 6, 2013 M_w 8.0 Santa Cruz Islands earthquake and tsunami. Tectonophysics 608, 1109–1121. http://dx.doi.org/10.1016/j.tecto.2013.07.001.

Lay, T., Ye, L., Kanamori, H., Yamazaki, Y., Cheung, K.F., Koper, K.D., Kwong, K., 2013b. The October 28, 2012 M_w 7.8 Haida Gwaii underthrusting earthquake and tsunami: slip partitioning along the Queen Charlotte Fault transpressional plate boundary. Earth Planet. Sci. Lett. 375, 57–70. http://dx.doi.org/10.1016/j.epsl.2013.05.005.

Lay, T., Yue, H., Brodsky, E.E., An, C., 2014. The 1 April 2014 Iquique, Chile, M_w 8.1 earthquake rupture sequence. Geophys. Res. Lett. 41, 3818–3825. http://dx.doi.org/10.1002/2014GL060238.

Lee, S.-J., 2011. Rupture process of the 2011 Tohoku-oki earthquake based upon joint source inversion of teleseismic and GPS data. Terr. Atmos. Ocean. Sci. 23, 1–7.

Lin, Y.N.N., et al., 2013. Coseismic and postseismic slip associated with the 2010 Maule Earthquake, Chile: characterizing the Arauco Peninsula barrier effect. J. Geophys. Res. 118. http://dx.doi.org/10.1002/jgrb.50207.

Lorito, S., Romano, F., Atzori, S., Tong, X., Avallone, A., McCloskey, J., Boschi, E., Piatanesi, A., 2011. Limited overlap between the seismic gap and coseismic slip of the great 2010 Chile earthquake. Nat. Geosci. 4, 173–177.

Loveless, J.P., Meade, B.J., 2010. Geodetic imaging of plate motions, slip rates, and partitioning of deformation in Japan. J. Geophys. Res. 115, B02410. http://dx.doi.org/10.1029/2008JB006248.

Maeda, T., Furumura, T., Sakai, S., Shinohara, M., 2011. Significant tsunami observed at ocean-bottom pressure gauges during the 2011 off the Pacific coast of Tohoku earthquake. Earth Planets Space 63, 803–808. http://dx.doi.org/10.5047/eps.2011.06.005.

Marone, C., Scholz, C., 1988. The depth of seismic faulting and the upper transition from stable to unstable slip regimes. Geophys. Res. Lett. 15, 621–624.

McCloskey, J., Antonioli, A., Piatanesi, A., Sieh, K., Steacy, S., Nalbant, S., Cocco, M., Giunchi, C., Huan, J., Dunlop, P., 2008. Tsunami threat in the Indian Ocean from a future megathrust earthquake west of Sumatra. Earth Planet. Sci. Lett. 265, 61–81. http://dx.doi.org/10.1016/j.epsl.2007.09.034.

Meltzner, A.J., Sieh, K., Chiang, H.-W., Shen, C.-C., Suwargadi, B.W., Natawidjaja, D.H., Philibosian, B., Briggs, R.W., 2012. Persistent termini of 2004-and 2005-like ruptures in the Sunda megathrust. J. Geophys. Res. 117, B04405. http://dx.doi.org/10.1029/2011JB008888.

Meng, L., Inbal, A., Ampuero, J.-P., 2011. A window into the complexity of the dynamic rupture of the 2011 M_w 9 Tohoku-oki earthquake. Geophys. Res. Lett. 38, L00G07. http://dx.doi.org/10.1029/2011GL048118.

Meng, L., Ampuero, J.-P., Stock, J., Duputel, Z., Luo, Y., Tsai, V.C., 2012. Earthquake in a maze: compressional rupture branching during the 2012 M_w 8.6 Sumatra earthquake. Science 336, 1118–1119.

Métois, M., Socquet, A., Vigny, C., 2012. Interseismic coupling, segmentation and mechanical behavior of the central Chile subduction zone. J. Geophys. Res. 117, B03406. http://dx.doi.org/10.1029/2011JB008736.

Michael, A.J., 2011. Random variability explains apparent global clustering of large earthquakes. Geophys. Res. Lett. 38, L21301.

Moreno, M., Rosenau, M., Oncken, O., 2010. 2010 Maule earthquake slip correlates with pre-seismic locking of Andean subduction zone. Nature 467, 198–202. http://dx.doi.org/10.1038/nature09349.

Moreno, M., Melnick, D., Rosenau, M., Baez, J., Klotz, J., Oncken, O., Hase, H., 2012. Toward understanding tectonic control on the M_w 8.8 2010 Maule Chile earthquake. Earth Planet. Sci. Lett. 321–322, 152–165. http://dx.doi.org/10.1016/j.epsl.2012.01.006.

Motagh, M., Wang, R., Walter, T.R., Bürgmann, R., Fielding, E., Anderssohn, J., Zschau, J., 2008. Coseismic slip model of the 2007 August Pisco earthquake (Peru) as constrained by wide swath radar observations. Geophys. J. Int. 174, 842–848.

Natawidjaja, D.H., Sieh, K., Chlieh, M., Galetzka, J., Suwargadi, B.W., Cheng, H., Edwards, R.L., Avouac, J.-P., Ward, S.N., 2006. Source parameters of the great Sumatran megathrust earthquakes of 1797 and 1833 inferred from coral microatolls. J. Geophys. Res. 111, B06403. http://dx.doi.org/10.1029/2005JB004025.

Newman, A.V., Hayes, G., Wei, Y., Convers, J., 2011. The 25 October 2010 Mentawai tsunami earthquake, from real-time discriminants, finite-fault rupture, and tsunami excitation. Geophys. Res. Lett. 38, L05302. http://dx.doi.org/10.1029/2010GL046498.

Nishenko, S.P., 1991. Circum-Pacific seismic potential: 1989–1999. Pure Appl. Geophys. 135, 169–259.

Nishimura, T., Hirasawa, T., Miyazaki, S., Sagiya, T., Tada, T., Miura, S., Tanaka, K., 2004. Temporal change of interplate coupling in northeastern Japan during 1995–2002 estimated from continuous GPS observations. Geophys. J. Int. 157 (2), 901–916.

Ozawa, S., Nishimura, T., Suito, H., Kobayahi, T., Tobita, M., Imakiire, T., 2011. Coseismic and postseismic slip of the 2011 magnitude-9 Tohoku-oki earthquake. Nature 475, 373–376. http://dx.doi.org/10.1038/nature10227.

Parsons, T., Geist, E.L., 2012. Were global $M \geq 8.3$ earthquake time intervals random between 1900 and 2011? Bull. Seismol. Soc. Am. 102 (40), 1583–1592. http://dx.doi.org/10.1785/0120110282.

Parsons, T., Velasco, A.A., 2011. Absence of remotely triggered large earthquakes beyond the mainshock region. Nat. Geosci. 4, 312–316.

Pelayo, A.M., Wiens, D.A., 1992. Tsunami earthquakes: slow thrust-faulting events in the accretionary wedge. J. Geophys. Res. 97, 15321–15337.

Poisson, B., Oliveros, C., Pedreros, R., 2011. Is there a best source model of the Sumatra 2004 earthquake for simulating the consecutive tsunami? Geophys. J. Int. 185, 1365–1378. http://dx.doi.org/10.1111/j.1365-246X.2011.05009.x.

Pollitz, F., Bürgmann, R., Banerjee, P., 2011a. Geodetic slip model of the 2011 M9.0 Tohoku earthquake. Geophys. Res. Lett. 38, L00G08. http://dx.doi.org/10.1029/2011GL048632.

Pollitz, F.F., Brooks, B., Tong, X., Bevis, M.G., Foster, J.H., Bürgmann, R., et al., 2011b. Coseismic slip distribution of the February 27, 2010 M_w 8.8 Maule, Chile earthquake. Geophys. Res. Lett. 38, L09309. http://dx.doi.org/10.1029/2011GL047065.

Pollitz, F.F., Stein, R.S., Sevilgen, V., Bürgmann, R., 2012. The 11 April 2012 east Indian Ocean earthquake triggered large aftershocks worldwide. Nature 490, 250–253. http://dx.doi.org/10.1038/nature11504.

Pritchard, M.E., Fielding, E.J., 2008. A study of the 2006 and 2007 earthquake sequence of Pisco, Peru, with InSAR and teleseismic data. Geophys. Res. Lett. 35, L09308. http://dx.doi.org/10.1029/2008GL033374.

Pritchard, M.E., Norabuena, E.O., Ji, C., Boroschek, R., Comte, D., Simons, M., Dixon, T.H., Rosen, P.A., 2007. Geodetic, teleseismic, and strong motion constraints on slip from recent southern Peru subduction zone earthquakes. J. Geophys. Res. 112, B03307. http://dx.doi.org/10.1029/2006JB004294.

Raeesi, M., Atakan, K., 2009. On the deformation cycle of a strongly coupled plate interface: the triple earthquakes of 16 March 1963, 15 November 2006, and 13 January 2007 along the Kurile subduction zone. J. Geophys. Res. 114, B10301. http://dx.doi.org/10.1029/2008JB006184.

Rhie, J., Dreger, D., Burgmann, R., Romanowicz, B., 2007. Slip of the 2004 Sumatra–Andaman earthquake from joint inversion of long-period global seismic waveforms and GPS static offsets. Bull. Seismol. Soc. Am. 97 (1A), S115–S127.

Ritsema, J., Lay, T., Kanamori, H., 2012. The 2011 Tohoku earthquake. Elements 8, 183–188. http://dx.doi.org/10.2113/gselements.8.3.183.

Robinson, D.P., 2011. A rare great earthquake on an oceanic fossil fracture zone. Geophys. J. Int. 186 (3), 1121–1134. http://dx.doi.org/10.1111/j.1365-246X.2011.05092.x.

Robinson, D.P., Das, S., Watts, A.B., 2006. Earthquake rupture stalled by a subducting fracture zone. Science 312, 1203–1205.

Ruiz, S., Metois, M., Fuenzalida, A., Ruiz, J., Leyton, F., Grandin, R., Vigny, C., Madariaga, R., Campos, J., 2014. Intense foreshocks and a slow slip event preceded the 2014 Iquique M_w 8.1 earthquake. Science. http://dx.doi.org/10.1126/science.1256074.

Satake, K., Fujii, Y., Harada, T., Namegaya, Y., 2013. Time and space distribution of coseismic slip of the 2011 Tohoku earthquake inferred from tsunami waveform data. Bull. Seismol. Soc. Am. 103, 1473–1492. http://dx.doi.org/10.1785/0120120122.

Scholz, C.H., 1998. Earthquakes and friction laws. Nature 391, 37–42.

Schurr, B., Asch, G., Hainzl, S., Bedford, J., Hoechner, A., Palo, M., Wang, R., Moreno, M., Bartsch, M., Zhang, Y., Oncken, O., Tilmann, F., Dahm, T., Victor, P., Barrientos, S., Vilotte, J.-P., 2014. Gradual unlocking of plate boundary controlled initiation of the 2014 Iquique earthquake. Nature. http://dx.doi.org/10.1038/nature13681.

Shao, G., Li, X., Ji, C., Maeda, T., 2011. Focal mechanism and slip history of the 2011 Mw 9.1 off the Pacific coast of Tohoku Earthquake, constrained with teleseismic body and surface waves. Earth Planets Space 63, 559–564. http://dx.doi.org/10.5047/eps.2011.06.028.

Shearer, P.M., Bürgmann, R., 2010. Lessons learned from the 2004 Sumatra–Andaman megathrust rupture. Annu. Rev. Earth Planet. Sci. 38, 103–131. http://dx.doi.org/10.1146/annurev-earth-040809-152537.

Shearer, P.M., Stark, P.B., 2012. Global risk of big earthquakes has not recently increased. Proc. Natl. Acad. Sci. 109 (3), 717–721.

Sieh, K., Natawidjajaj, D.H., Meltzner, A.J., Shen, C.-C., Cheng, H., Li, K.-S., Suwargadi, B.W., Galetzka, J., Philibosian, B., Edwards, R.L., 2008. Earthquake supercycles inferred from sea-level changes recorded in the corals of West Sumatra. Science 322, 1674–1678. http://dx.doi.org/10.1126/science.1163589.

Simons, M., Minson, S.E., Sladen, A., Ortega, F., Jiang, J., Owen, S.E., Meng, L., Ampuero, J.-P., Wei, S., Chu, R., et al., 2011. The 2011 magnitude 9.0 Tohoku-oki earthquake: mosaicking the megathrust from seconds to centuries. Science 332, 1421–1425.

Sladen, A., Tavera, H., Simons, M., Avouac, J.P., Konca, A.O., Perfettini, H., Audin, L., Fielding, E.J., Ortega, F., Cavagnoud, R., 2010. Source model of the 2007 M_w 8.0 Pisco, Peru earthquake: implications for seismogenic behavior of subduction megathrusts. J. Geophys. Res. 115, B02405. http://dx.doi.org/10.1029/2009JB006429.

Steblov, G.M., Kogan, M.G., Levin, B.V., Vasilenko, N.F., Prytkov, A.S., Frolov, D.I., 2008. Spatially linked asperities of the 2006–2007 great Kuril earthquakes revealed by GPS. Geophys. Res. Lett. 35, L22306. http://dx.doi.org/10.1029/2008GL035572.

Suwa, Y., Miura, S., Hasegawa, A., Sato, T., Tachibana, K., 2006. Interplate coupling beneath NE Japan inferred from three-dimensional displacement field. J. Geophys. Res. 111 (B4). http://dx.doi.org/10.1029/2004JB003203.

Taylor, W., Briggs, R.W., Frohlich, C., Brown, A., Hornbach, M., Papabatu, A.K., Metzner, A.J., Bily, D., 2008. Rupture across arc segment and plate boundaries in the 1 April 2007 Solomons earthquake. Nat. Geosci. 1, 253–257. http://dx.doi.org/10.1038/ngeo159.

Thenhaus, P.C., Campbell, K.W., Khater, M.M., 2011. Spatial and temporal earthquake clustering: part 1. Global earthquake clustering. White paper, EQECAT.

Tong, X., Sandwell, D., Luttrell, K., Brooks, B., Bevis, M., Shimada, M., et al., 2010. The 2010 Maule, Chile earthquake: downdip rupture limit revealed by space geodesy. Geophys. Res. Lett. 37, L24311. http://dx.doi.org/10.1029/2010GL045805.

Uchida, N., Matsuzawa, T., 2011. Coupling coefficient, hierarchical structure, and earthquake cycle for the source area of the 2011 Tohoku earthquake inferred from small repeating earthquake data. Earth Planets Space 63, 675–679. http://dx.doi.org/10.5047/eps.2011.07.006.

van der Elst, N.J., Brodsky, E.E., Lay, T., 2013. Remote triggering not evident near epicenters of impending great earthquakes. Bull. Seismol. Soc. Am. 103, 1522–1540. http://dx.doi.org/10.1785/0120120126.

Velasco, A.A., Hernandez, S., Parsons, T., Pankow, K., 2008. Global ubiquity of dynamic earthquake triggering. Nat. Geosci. 1, 375–379.

Vigny, C., Simons, W.J.F., Abu, S., Bamphenyu, R., Satirapod, C., Choosakul, N., Subarya, C., Socquet, A., Omar, K., Abidin, H.Z., Ambrosius, B.A.C., 2005. Insight into the 2004 Sumatra–Andaman earthquake from GPS measurements in southeast Asia. Nature 436, 201–206.

Vigny, C., Socquet, A., Peyrat, S., Ruegg, J.-C., Metois, M., Madariaga, R., et al., 2011. The 2010 M_w 8.8 Maule mega-thrust earthquake of central Chile, monitored by GPS. Science 332, 1417–1421.

Walker, K.T., Ishii, M., Shearer, P.M., 2005. Rupture details of the 28 March 2005 Sumatra M_w 8.6 earthquake imaged with teleseismic P waves. Geophys. Res. Lett. 32, L24303. http://dx.doi.org/10.1029/2005GL024395.

Wang, D., Mori, J., 2011a. Rupture process of the 2011 off the Pacific coast of Tohoku earthquake (M_w 9.0) as imaged with back-projection of teleseismic P waves. Earth Planets Space 63, 603–607. http://dx.doi.org/10.5047/eps.2011.05.029.

Wang, D., Mori, J., 2011b. Frequency-dependent energy radiation and fault coupling for the 2010 M_w 8.8 Maule, Chile and 2011 M_w 9.0 Tohoku, Japan earthquakes. Geophys. Res. Lett. 38, L22308. http://dx.doi.org/10.1029/2011GL049652.

Wei, S., Helmberger, D., Avouac, J.-P., 2013a. Modeling the 2012 Wharton basin earthquakes off-Sumatra: complete lithospheric failure. J. Geophys. Res. 118, 3592–3609. http://dx.doi.org/10.1002/jgrb.50267.

Wei, S., Helmberger, D., Zhan, Z., Graves, R., 2013b. Rupture complexity of the Mw 8.3 Sea of Okhotsk earthquake: rapid triggering of complementary earthquakes? Geophys. Res. Lett. 40, 1–6. http://dx.doi.org/10.1002/grl.50977.

West, M., Sanchez, J.J., McNutt, S.R., 2005. Periodically triggered seismicity at Mount Wrangell, Alaska, after the Sumatra earthquake. Science 308, 1144–1146.

Xu, Y., Koper, K.D., Sufri, O., Zhu, L., Hutko, A.R., 2009. Rupture imaging of the M_w 7.9 12 May 2008 Wenchuan earthquake from back projection of teleseismic P waves. Geochem. Geophys. Geosyst. 10, Q04006. http://dx.doi.org/10.1029/2008GC002335.

Yamazaki, Y., Lay, T., Cheung, K.F., Yue, H., Kanamori, H., 2011. Modeling near-field tsunami observations to improve finite-fault slip models for the 11 March 2011 Tohoku earthquake. Geophys. Res. Lett. 38, L00G15. http://dx.doi.org/10.1029/2011GL049130.

Yamazaki, Y., Cheung, K.F., Lay, T., 2013. Generation mechanism and near-field dynamics of the 2011 Tohoku tsunami. Bull. Seismol. Soc. Am. 103, 1444–1455. http://dx.doi.org/10.1785/0120120103.

Yao, H., Gerstoft, P., Shearer, P.M., Mecklenbrauker, C., 2011. Compressive sensing of the Tohuku-Oki M_w 9.0 earthquake: frequency-dependent rupture modes. Geophys. Res. Lett. 38. http://dx.doi.org/10.1029/2011GL049223.

Ye, L., Lay, T., Kanamori, H., 2013a. Ground shaking and seismic source spectra for large earthquakes around the megathrust fault offshore of Honshu, Japan. Bull. Seismol. Soc. Am. 103, 1221–1241. http://dx.doi.org/10.1785/0120120115.

Ye, L., Lay, T., Kanamori, H., 2013b. Large earthquake rupture process variations on the Middle America megathrust. Earth Planet. Sci. Lett. 381, 147–155.

Ye, L., Lay, T., Kanamori, H., Koper, K.D., 2013c. Energy release of the 2013 M_w 8.3 Sea of Okhotsk earthquake and deep slab stress heterogeneity. Science 341, 1380–1384.

Yokota, Y., Koketsu, K., Fujii, Y., Satake, K., Sakai, S., Shinohara, M., Kanazawa, T., 2011. Joint inversion of strong motion, teleseismic, geodetic, and tsunami datasets for the rupture process of the 2011 Tohoku earthquake. Geophys. Res. Lett. 38, L00G21. http://dx.doi.org/10.1029/2011GL050098.

Yoshida, Y., Ueno, H., Muto, D., Aoki, S., 2011. Source process of the 2011 off the Pacific coast of Tohoku earthquake with the combination of teleseismic and strong motion data. Earth Planets Space 63, 565–569. http://dx.doi.org/10.5047/eps.2011.05.011.

Yue, H., Lay, T., 2011. Inversion of high-rate (1-sps) GPS data for rupture process of the 11 March 2011 Tohoku earthquake (M_w 9.1). Geophys. Res. Lett. 38, L00G09. http://dx.doi.org/10.1029/2011GL048700.

Yue, H., Lay, T., 2013. Source rupture models for the M_w 9.0 2011 Tohoku earthquake from joint inversions of high-rate geodetic and seismic data. Bull. Seismol. Soc. Am. 103, 1242–1255. http://dx.doi.org/10.1785/0120120119.

Yue, H., Lay, T., Koper, K.D., 2012. *En échelon* and orthogonal fault ruptures of the 11 April 2012 great intraplate earthquakes. Nature 490, 245–249. http://dx.doi.org/10.1038/nature11492.

Yue, H., Lay, T., Schwartz, S.Y., Rivera, L., Protti, M., Dixon, T.H., Owen, S., Newman, A.V., 2013. The 5 September 2012 Nicoya, Costa Rica M_w 7.6 earthquake rupture process from joint inversion of high-rate GPS, strong-motion, and teleseismic *P*

wave data and its relationship to adjacent plate boundary interface properties. J. Geophys. Res. 118, 5453–5466. http://dx.doi.org/10.1002/jgrb.50379.

Yue, H., Lay, T., Rivera, L., Bai, Y., Yamazaki, Y., Cheung, K.F., Hill, E.M., Sieh, K., Kongko, W., Muhari, A., 2014a. Rupture process of the 2010 M_w 7.8 Mentawai tsunami earthquake from joint inversion of near-field hr-GPS and teleseismic body wave recordings constrained by tsunami observations. J. Geophys. Res. 119, 5574–5593. http://dx.doi.org/10.1002/2014JB011082.

Yue, H., Lay, T., Rivera, L., An, C., Vigny, C., Tong, X., Báez Soto, J.C., 2014b. Localized fault slip to the trench in the 2010 Maule, Chile $M_w = 8.8$ earthquake from joint inversion of high-rate GPS, teleseismic body waves, InSAR, campaign GPS, and tsunami observations. J. Geophys. Res. 119. http://dx.doi.org/10.1002/2014JB011340.

Zhang, H., Ge, Z., Ding, L., 2011. Three sub-events composing the 2011 off the Pacific coast of Tohoku Earthquake (M_w 9.0) inferred from rupture imaging by back-projecting teleseismic P waves. Earth Planets Space 63, 595–598. http://dx.doi.org/10.5047/eps.2011.06.021.

Zhao, D., Huang, Z., Umino, N., Hasegawa, A., Kanamori, H., 2011. Structural heterogeneity in the megathrust zone and mechanism of the 2011 Tohoku-oki earthquake (M_w 9.0). Geophys. Res. Lett. 38, L17308. http://dx.doi.org/10.1029/2011GL048408.

Thorne Lay is Distinguished Professor of Earth and Planetary Sciences at the University of California Santa Cruz, where he has been located since 1990. Previously he was a faculty member at the University of Michigan, after receiving his Ph.D. in Geophysics from the California Institute of Technology in 1983. His research area is seismology, and includes studies of large earthquake ruptures, internal structure of the Earth, and application of seismology to support monitoring of nuclear testing treaties. He is author or co-author of 411 research publications including 5 books, 286 publications in refereed books and professional journals, and 120 technical reports, book reviews, news items and conference proceedings. He is an elected Fellow of the National Academy of Sciences, the American Academy of Arts and Sciences, and the American Association for the Advancement of Sciences. He has received the Inge Lehmann Medal of the American Geophysical Union, the Harry Fielding Reid Medal of the Seismological Society of America and the Macelwane Medal of the American Geophysical Union.